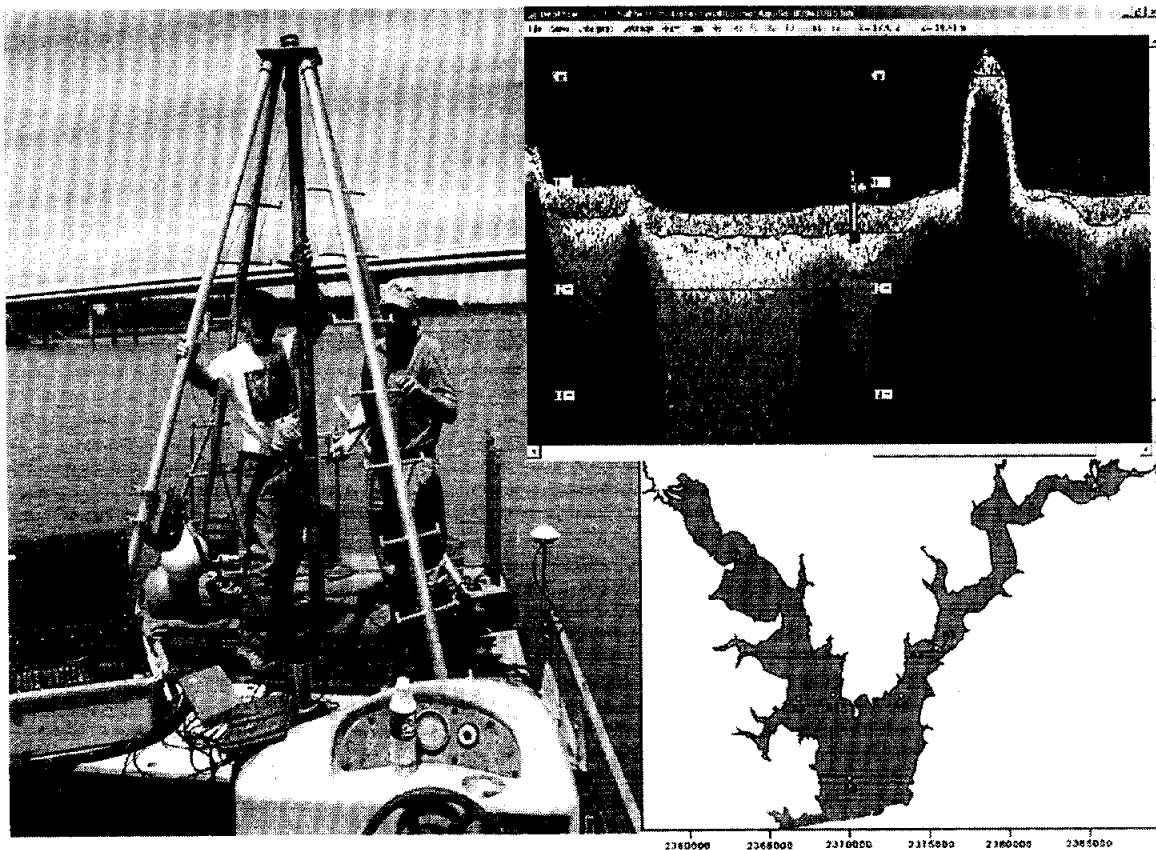


Baylor University

Department of Geology

**Baylor University
Department of Geology
PO Box 979354
Waco, TX 76798-7354**

**Sediment Thickness from Coring and Acoustics within
Lakes Aquilla, Granger, Limestone, and Proctor:
Brazos River Watershed, TX**



By John A. Dunbar and Peter M. Allen

June 2003

EXECUTIVE SUMMARY

The goal of this study was to determine the extent to which the thickness of post-impoundment sediments in water reservoirs of the Brazos River Basin can be measured and mapped using a multi-frequency acoustic profiling system made by Specialty Devices, Inc. (SDI) of Plano, Texas. To this end we collected 35 cores from 23 locations in four reservoirs in the Brazos River Basin (Lakes Aquilla, Granger, Limestone, and Proctor). The cores were collected using the vibracore technique and ranged in length from 5 cm to 3 m. The pre-impoundment surface was reached and sampled on all but one of these locations. At that location the bottom had apparently been exposed and dried at some point in the past. One core from each location was sliced in 5 cm sub-samples. The sub-samples were all visually examined, and analyzed for water content and sediment shear strength. Texture analysis to determine the percentage of sand, silt and clay was performed on the sub-samples of selected cores from each reservoir. We found that in the four reservoirs the pre-impoundment surface was distinct and easily identified in all the cores collected on the submerged floodplains. Pre-impoundment materials are characterized by low water content (25 to 35% water content versus 50 to 80% water content for the post-impoundment sediments), high shear strength (1 to 2 kg/cm² versus 0.05 to 0.5 kg/cm² for the post-impoundment sediment) and the common presence of tree bark, twigs and leaf litter on the pre-impoundment surface and intact plant roots within the soil immediately below the pre-impoundment surface. The distinction between pre- and post-impoundment sediment is not as great in cores collected in the submerged river channels. The water content and shear strength of the lake and river deposits differ, but the differences are more subtle than those found on the floodplain. Generally the lake and river channel sediments have similar textures and appearance.

The correlation between the cores and the acoustic data was achieved in two ways. First, short acoustic records were collected using the SDI profiling system while still at anchor at each core site. For the second form of correlation, continuous acoustic profiles were collected through the core sites. On the short acoustic records the post-impoundment layer appears white to yellow, with specks of red on three-color displays generated by the interpretation program provided with the SDI system. The underlying pre-impoundment material in all four reservoirs, whether it was alluvium, colluvium, or river channel deposits, appears light to dark blue on the three-color displays. On single frequency displays of the 48 kHz acoustic data, the post-impoundment layer appears light gray and the pre-impoundment has a black and white speckled pattern. Thickness estimated from acoustic data agree with the core results to within 5 cm, assuming a sediment velocity of 1440 m/s (4,723 ft/s). The profiling results show that the post-impoundment layer produces a distinct acoustic response that is easily traced on acoustic profiles in all four reservoirs. Although it would be possible to reliably identify and map the base of the post-impoundment sediments without guidance from core data, having results from coring provides a useful conformation that the correct surface is being mapped.

ACKNOWLEDGEMENTS

We gratefully acknowledge the technical assistance of Paul Higley, who joined us on two coring trips and Heidi Henson, who helped with the core analysis. Financial support was provided by the Texas Water Development Board and the Brazos River Authority.

Author contact information:

John A. Dunbar, Department of Geology, Baylor University, P.O. Box 97354, Waco, TX 76798-7354, (254) 710-2361, john_dunbar@baylor.edu

Peter M. Allen, Department of Geology, Baylor University, P.O. Box 97354, Waco, TX 76798-7354, (254) 710-2361, peter_allen@baylor.edu

1. INTRODUCTION

In the Spring of 2002 the Texas Water Development Board (TWDB) purchased an acoustic water reservoir sediment survey system from Specialty Devices, Inc. of Plano Texas (SDI). The system was originally developed in a collaborative project between Baylor University and SDI, funded by Texas Higher Education Coordinating Board Advanced Technology Program Grant 3545-006 (Dunbar et al., 1995). The goal of the project was to develop a water reservoir system that could produce accurate measures of both the water and sediment volume contained in reservoirs in a single survey. Since its original development, the commercialized version of the system has been used to survey large reservoirs (Dunbar et al., 1996; Dunbar et al, 2003), small flood control reservoirs (Dunbar et al., 2001; Bennett and Dunbar, 2003), as well as natural lakes, harbors, and rivers.

The SDI system differs from conventional acoustic surveying systems in that it collects data in multiple signal frequency bands simultaneously. High-frequency signals (200 kilohertz) provide a sharp image of low-density mud at the water bottom, whereas lower-frequency signals (48 and 24 kilohertz) are used to image the base of sediment fill. Measuring the thickness of accumulated post-impoundment sediment is done by identifying and tracing the water bottom and the base of fill on the acoustic records. Because the water reservoir represents a distinctly different sedimentation environment than the river valley that preceded it, the acoustic response of sediments deposited in the reservoir is likely to be distinct from that of the pre-impoundment soils, alluvium and colluvium. Although, a traceable contrast between pre- and post-impoundment materials is reasonable to expect, it has not been extensively tested and verified by observation.

This is a preliminary report describing the results of direct comparisons between measurements of post-impoundment sediment thickness determined by coring and acoustic profiling in four reservoirs in the Brazos River watershed (Lakes Aquilla, Granger, Limestone, and Proctor). The study was done in connection with complete sediment surveys conducted in the same reservoirs by TWDB personnel in Fall 2002 and Spring 2003 and a third study comparing chemical and isotopic methods for identifying the pre-impoundment surface and the use of conventional sub-bottom profiling to trace the pre-impoundment surface by personnel from Texas A&M at Galveston.

3. PROCEDURES

The goal of the present study was to determine the extent to which the thickness of the pre-impoundment fill can be mapped within water reservoirs by the SDI acoustic profiling system. The approach taken was to use an independent method for directly measuring the depth below the reservoir bottom to the pre-impoundment surface at a limited number of points in four example reservoirs. The direct measurement of sediment thickness was done by collecting continuous undisturbed cores using a vibracore device. The correlation between the cores and the acoustic data was achieved in two ways. First, short acoustic records were collected using the same model SDI profiling system as that owned by the TWDB, while still at anchor at each core site. Because the survey boat remained anchored at the core site, these short records image the bottom at points only a few feet away from where the core tube penetrated the bottom. For

the second form of correlation, the geographic locations of the core sites were determined to sub-meter accuracy using differential GPS positioning before leaving the site. Then, with the survey boat underway, continuous acoustic profiles were collected through the core sites. While the core and acoustic data are not as closely correlated in these continuous profiles, they are valuable in that they show the core in respect to the variability along the entire transect across the reservoirs.

2.1 Sediment Coring

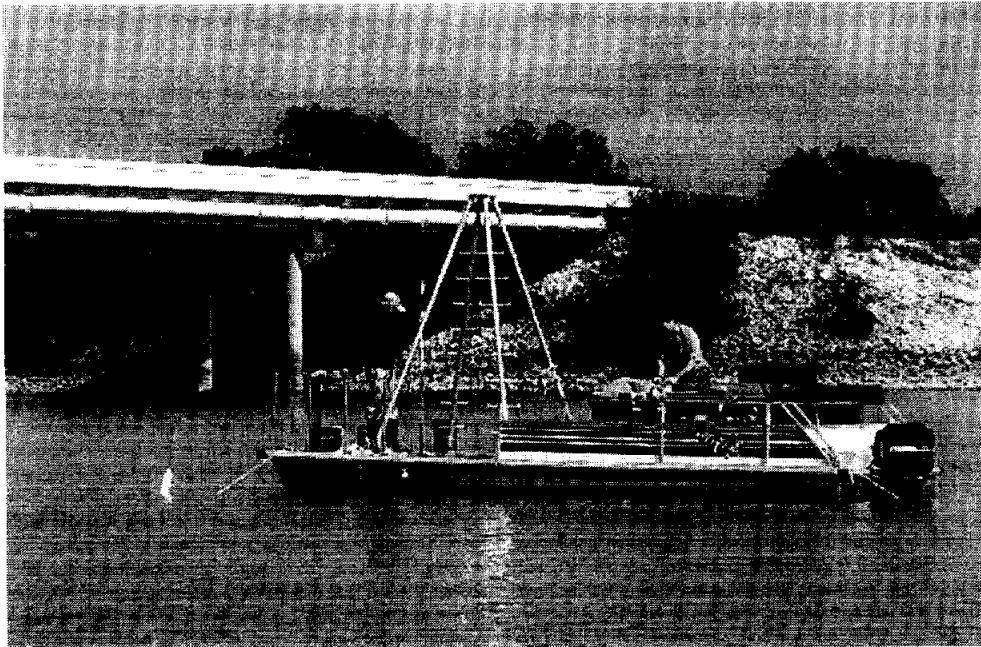
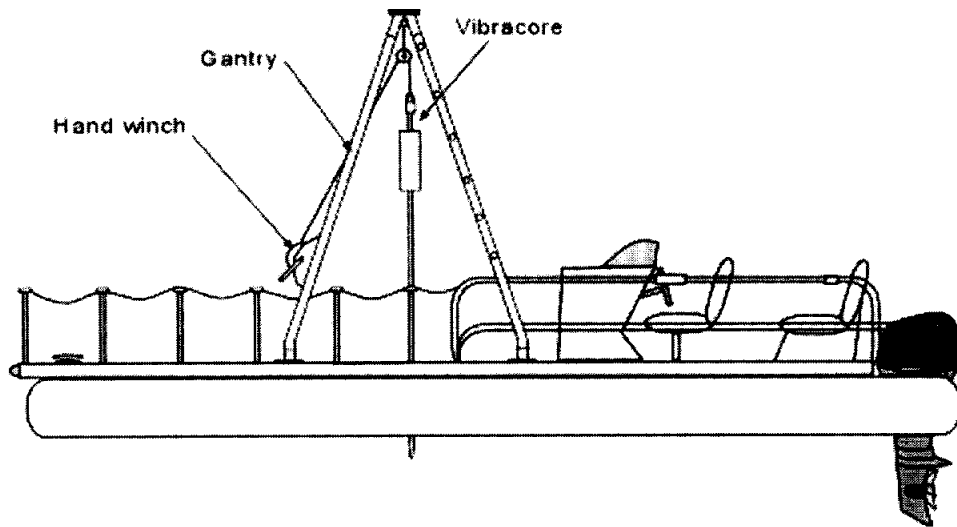
A vibracoring system commercially available from SDI was used to core sediments within the four test lakes considered in this study Lake (Figures 2-1, 2.-2). Vibracoring is a common approach for obtaining undisturbed cores of unconsolidated sediment in saturated or nearly saturated conditions (Lanesky et al., 1979; Smith, 1984). The SDI vibracore uses a 1-HP motor that drives a pair of weights that are eccentrically mounted on two counter rotating shafts. The motor and vibrator mechanism is housed within a watertight aluminum chamber so it can be immersed in water (Figure 2-2). The chamber is connected to the top of an aluminum irrigation tube, with 1.5-mm wall thickness and 76-mm (3 in.) diameter or a clear acrylic tube of the same diameter (as shown) that is cabled to a 2.5-m tall aluminum gantry fitted with a hand-operated winch. The vibracore driver is powered by two 12-volt batteries connected in series through a 125-ft power cord, thus limiting the depth of operation. Lengths of core tube 4 to 12 ft (1.2 to 3.7 m) long were used. The gantry is mounted on a 24 ft pontoon boat that has a 4 ft square "moon" pool cut into its deck (Figures 2-1).

The goal in choosing core locations was to collect cores that represent each sedimentary environment encountered in acoustic surveys. Generally, within reservoirs, fine-grained sediments tend to be transported further toward the dam than coarse-grained sediments. At a given position along the axis of reservoirs more sediment is normally deposited within the submerged stream axis than on the submerged floodplain. Hence, in locating core sites, we attempted to collect cores within submerged stream channels and adjacent submerged floodplains, both near the dam and upstream on the major arms of each reservoir. The exact core sites were chosen in the field, by using the acoustic profiling system to find the submerged stream axis. Once the stream was found, the survey boat was anchored on site with three anchors spread at 120° intervals around the compass rose, with two 60° to either side of the wind direction and one directly downwind. When cores and short acoustic records were collected on the submerged stream channel, the anchors were pulled and the boat was moved to an adjacent point on the submerged floodplain. When cores had been collected at both sites, a profile was collected through the two sites.

Cores were collected by lowering the vibrator with core tube attached to the bottom by hand winch, switching on the vibrator, and allowing the tube to slowly vibrate into the bottom. The vibration causes the sediment to liquefy in region a few millimeters thick near the tube wall, allowing the tube to slide into the sediment with little drag. This results in less disturbance and compaction of the sediment cores than occurs with gravity-driven drop coring devices. When the core had reached the point of refusal, the vibrator was turned off and the core was winched out of the bottom. Once on deck, the retrieved cores were capped top and bottom with rubber end-caps and stored upright during transport (Figure 2-3). Long cores were sectioned into 4 ft lengths for transport and storage.

Cores from the submerged stream channels were normally collected with tubes 8 to 12 ft in length with aluminum core catchers epoxied into the lower end of the tubes (Figure 2-4). The cores collected in the submerged river channels easily penetrated the low-density post-impoundment fill and several meters of somewhat denser pre-impoundment fluvial deposits. The fluvial deposits were generally soft, and the core catchers were needed to keep the core in the tube during retrieval. The core catchers are made up of a series of fingers cut into thin aluminum sheets, which are bent into rings and glued into the ends of the core tubes. During coring, the fingers flatten against the inside of the tube as the core slides into the tube. Then during retrieval, the fingers bend out into the tube, preventing the core from sliding completely out of the tube.

Cores from the submerged floodplains were normally collected with tubes 4 to 6 ft in length without core catchers. The sediment accumulation on the submerged floodplains was normally less than 1 m and the compacted, clay-rich soils of the underlying floodplain formed a tight plug that held the core in the tube during retrieval. In nearly every case, cores from the submerged floodplains penetrate the entire post-impoundment sediment fill and sample the pre-impoundment soil, alluvium or colluvium.



a.

Figure 2-1. Coring boat with gantry. (a) Schematic diagram of 24 ft coring boat and vibracoring system. (b) Coring boat at Lake Aquilla.

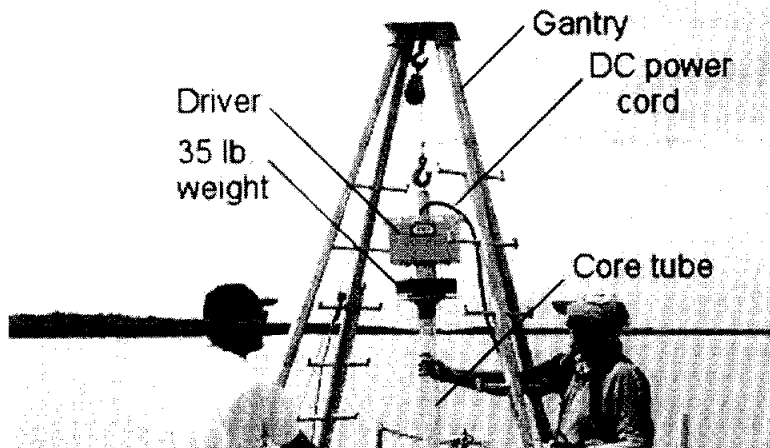


Figure 2-2. Picture of vibracorer with clear acrylic core tubing taken on Lake Aquilla.

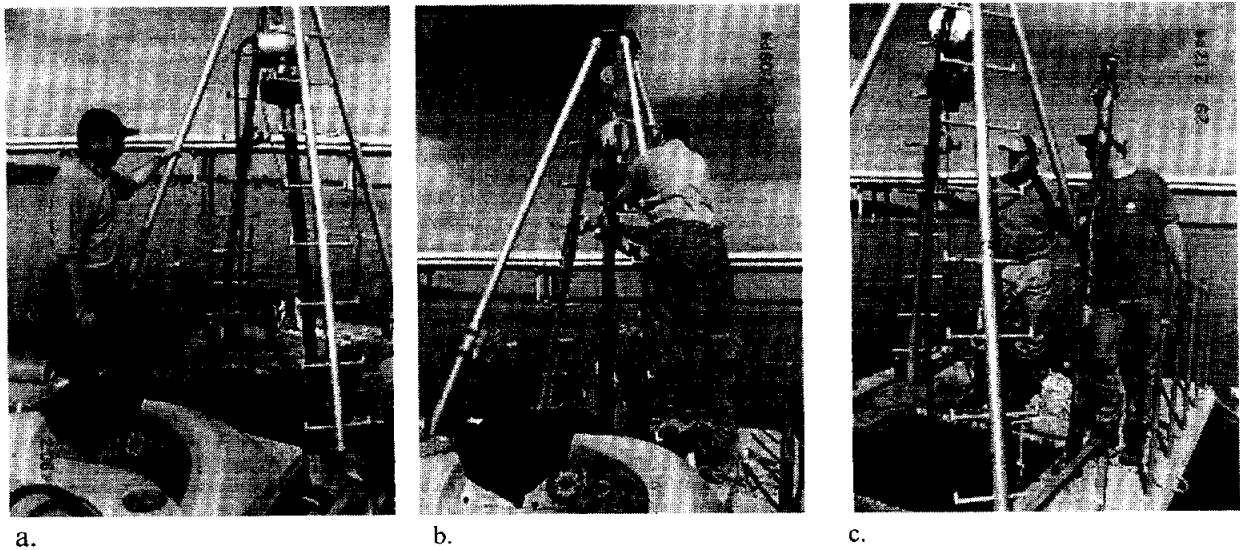


Figure 2-3. Recovering a core on Lake Aquilla. (a) Rubber end cap is placed on the base of the core as it comes out of the water in the moon pool. (b) Top of core is disconnected from the vibracorer driver. (c) End cap placed on the top of the 8 ft core.

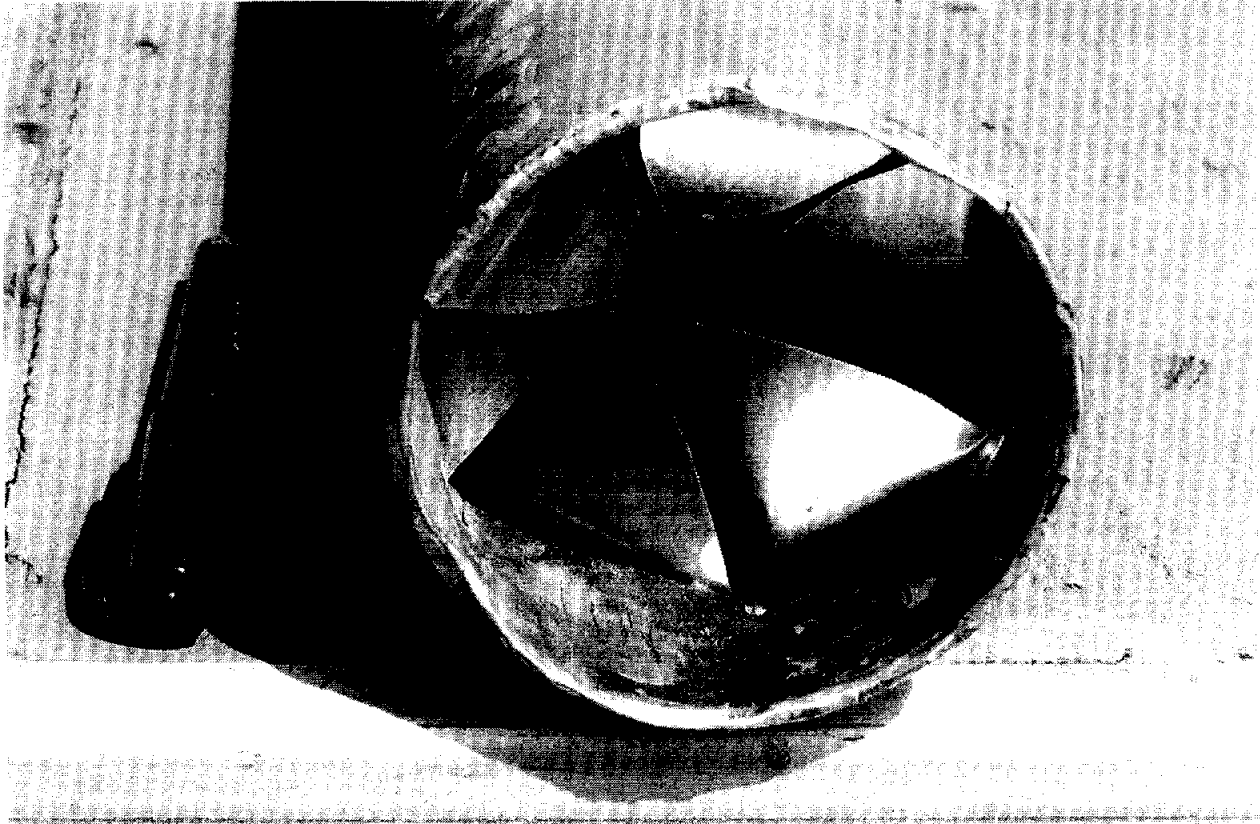


Figure 2-4. Core catcher epoxied into the end of a 12 ft long aluminum core tube. The core catcher holds the core in the tube during retrieval.

2.2 Core analysis:

The main goal of our core analysis was to determine the thickness of the post-impoundment sediment present in each core. A secondary goal was to determine the water content and texture variations in the cores to further refine the correlation with the acoustic data. In this analysis, we relied on visual examination of the sampled material, measurements of the water content and sediment strength in all cores, and sediment texture determinations within selected cores. After the cores were brought back from the field, they were refrigerated until they could be sub-sampled. The cores were sub-sampled by cutting the core tube and sediment into 5-cm slices using a pipe cutter (Figure 2-5). The sediment within each 5-cm slice was placed into pre-weighed containers, dried for 48 hours at 106° C, reweighed and stored for further analysis. The wet and dry weights of the samples were used to compute water content profiles along the cores. During the sub-sampling operation the strength of the sediment was determined using a pocket penetrometer that measures the force required to drive a 2.5 cm diameter disk into the sediment. These tests were performed on the top of each 5 cm sample, while the sample was confined in the core tube.

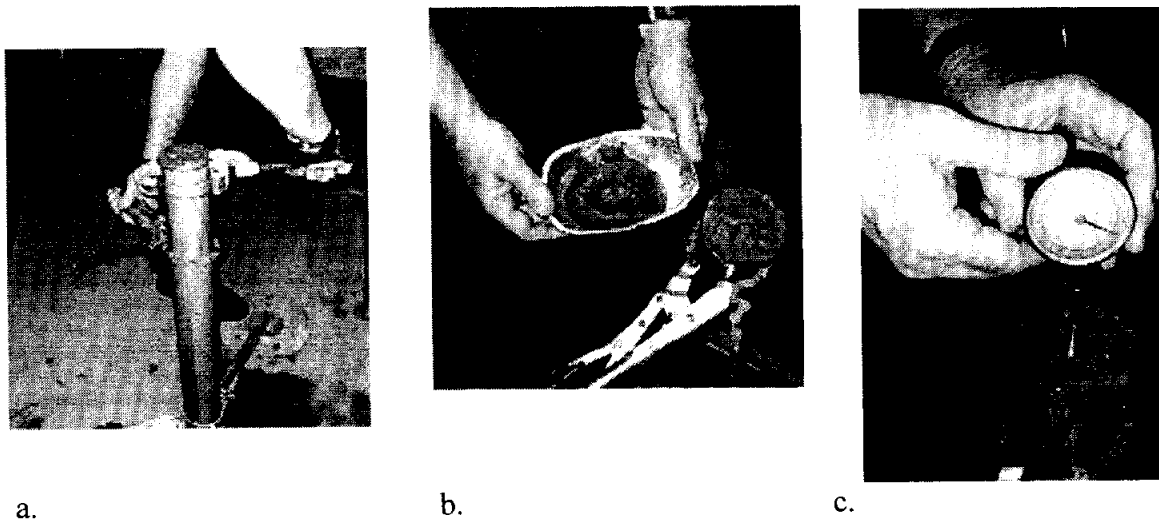


Figure 2-5. Sub-sampling of cores. (a) Sectioning core into 5 cm slices. (b) Example 5-cm sub-sample ready for drying. (c) Sediment shear strength measured using a penetration device.

2.3 Texture analysis

There are two standard approaches to texture analysis for grain sizes, those associated with sediments and those associated with soils. Both standard methods rely on sieving to separate and classify the sand and coarser fraction and settling velocity versus grain size to separate the silt and clay sizes. The main distinction between the sediment and soil approaches to texture

analysis is that sediment samples are done with wet samples and soil samples are completely dried before analysis begins. This difference is related to clays and their tendency to flocculate and mimic larger grains. Sediment samples are analyzed wet to avoid clay flocculation. This tends to over estimate the coarse fraction at the expense of the fine fraction. Soils normally go through several natural saturation and desiccation cycles each year and the samples are collected with widely varying states of saturation. All samples are dried completely before analysis, so that they start at the same state. There is little chance of inducing more flocculation by adding one more drying cycle. The texture analysis of reservoir fill is complicated by the fact that both sediments and soils are present. The one goal is to discriminate between the reservoir fill sediments and the underlying pre-impoundment soils. The problem is further complicated by the fact that the sediments within shallow parts of water reservoirs are commonly exposed and desiccated during periods of prolonged drought. If all the samples are treated as sediments, naturally flocculated clays will cause the coarse fraction to be over estimated in the previously desiccated sediments and pre-impoundment soils relative to the sediments that have never been dried. Hence, we treated all the samples following soils procedures (drying the samples initially so that all the samples would begin at the same state).

In addition to the standard methods of texture analysis there are several rapid methods useful for analyzing large number of samples in cores to see vertical trends. One method relies on measuring light scattered by sediment particles in suspension to determine size in a device called a sedigraph. Another method relies on measuring particle sizes visually on so-called "smear slides" viewed under a petrographic microscope. The advantage of the smear slide approach is that under the petrographic microscope quartz grains transmit light readily and appear white, yellow, or light blue, whereas clay and organic materials are nearly opaque. Hence, the discrimination between quartz sand and silt grains and flocculated clay and organic particles is not a problem. Smear slides are prepared by placing a small drop of sediment sample on a slide in a drop of water treated with PhotoFlow™ to disperse the particles. The sediment is then smeared over the slide into a thin, transparent layer using a glass rod (Figure 2-6). The slides are then dried on a hotplate and a slide cover is glued onto the smear with mounting medium. The slides are then examined under a petrographic microscope under cross-nickels using a quartz filter so that quartz grains appear white, yellow, or light blue, flocculated clay and organic material is opaque, and gaps between grains appear purple (Figure 2-7). The smear slides are normally analyzed in a semi-quantitative way, subjectively judging the percent sand, silt and clay present in each field of view point. To improve the accuracy of this process we scanned each microphotograph and did the counting numerically with custom image analysis software. The software identifies the grain material by color and the size by counting the number of pixels contained in each particle on the frame. The average count on six frames was computed for samples containing sand particles and the average of three frames was computed for samples containing only silt and clay.

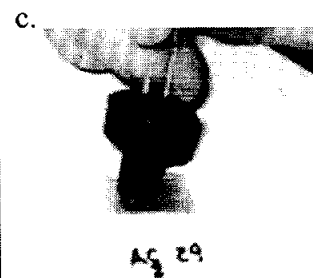
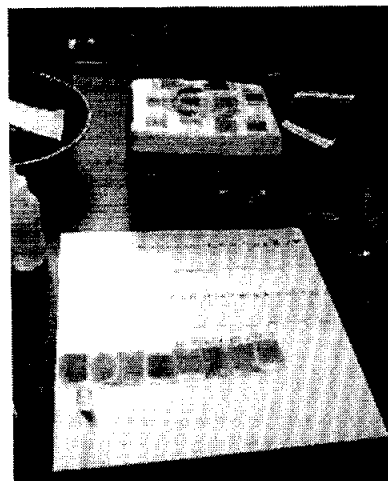
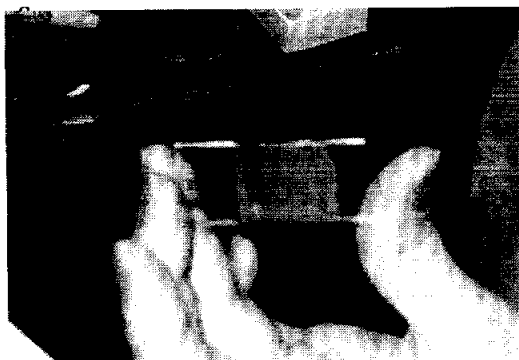


Figure 2-6. Preparation of a smear slide for texture analysis. (a) Sediment sample is smeared over a glass slide. (b) Smear slides are dried on a hot plate. (c) Slide cover is glued over sediment smear.

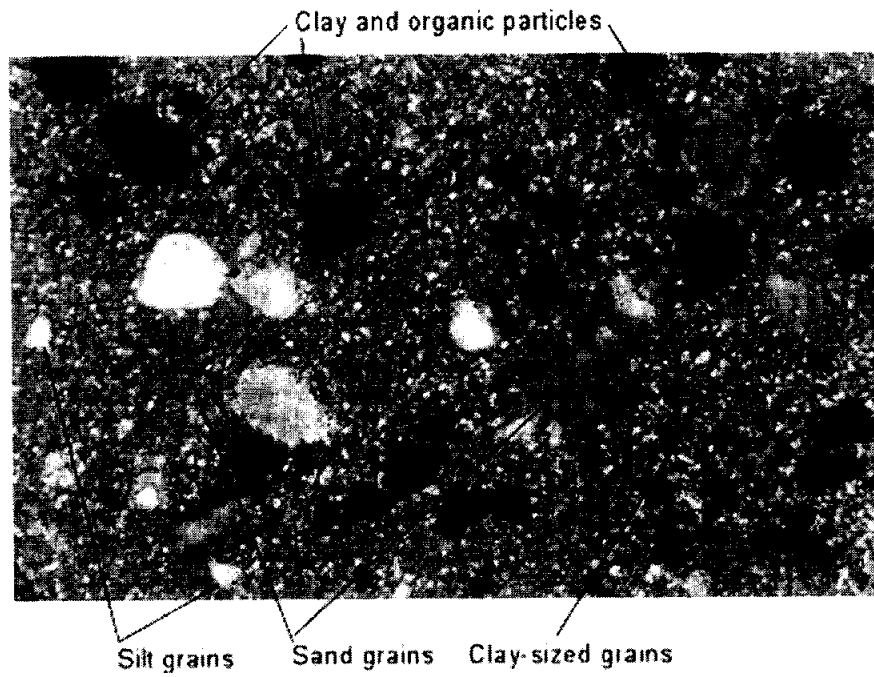


Figure 2-7. Photomicrograph of sediment smear. The field of view is 0.66 mm wide.

2.3 Discriminating Between Pre- and Post-impoundment materials

The overall goal of this project was to determine the thickness of post-impoundment sediment at a number of points in the four example reservoirs and to compare those thicknesses with the results of acoustical profiling. The extent to which one can discriminate the post-impoundment sediment (the sediment that has accumulated since the construction of the dam) from the pre-impoundment sediment (the sediment that was present prior to the construction of the dam in the cores) is the major question posed in this research. There are approaches to making this distinction based on isotopic dating methods. The sediments can be dated using radioactive lead (^{210}Pb ; 22-year half-life; Binford and Brenner, 1986) and compared to the date of impoundment. The sediments can also be analyzed for radioactive cesium (^{137}Cs ; 30-year half-life) to find sediments deposited at specific dates, which can be compared to the impoundment date. Because ^{137}Cs is produced during nuclear fission, its presence in the environment is due to nuclear testing or releases from nuclear reactors (Ritchie and McHenry, 1990). First global deposition of ^{137}Cs occurred in 1954 ± 2 and maximum deposition occurred in 1964 ± 2 in the Northern Hemisphere, related to above ground nuclear testing. In the current study these isotopic approaches to discriminating pre- and post-impoundment materials will be performed by personnel at Texas A&M Galveston.

In our work we made an independent interpretation of the depth to the pre-impoundment surface in each core based on the following evidence: (1) a visual examination of the core for obvious terrestrial materials, such as leaf litter, tree bark, twigs, grass roots, etc., concentrations of which would be expected on or just below the pre-impoundment surface, but not in the post-impoundment sediment and (2) variations in the physical properties of the sediment, particularly sediment water content, shear strength and texture with depth. Sediments deposited in reservoirs typically have water contents that range from 50 to 80% at the water bottom and decrease with burial to 30 to 40% at depths of several meters. Lower water contents occur where the bottom has been exposed and desiccated at some point. Sediments that have been desiccated and re-saturated never return to their original high water content. Soils, in contrast, typically have water contents of 20 to 30% when saturated. The shear strength of reservoir sediments (as measured with penetration devices) typically ranges from 0 to 1.0 kg/cm^2 . The shear strength of saturated clay-rich soils typically ranges from 3 to over 10 kg/cm^2 .

2.4 Acoustic Profiling

The acoustic profiling system used in this study is the same SDI profiler model as that used by the TWDB in its sediment surveys. The system images the bottom and sub-bottom sediments with acoustic transducers with central frequencies of 200, 48, and 24 kHz (Figure 2-8, 2-9). During acquisition, the system collects traces using each transducer independently in a rapid, round-robin succession. The high-frequency signals provide a sharp image of low-density mud at the water bottom, whereas the low-frequency signals penetrate many meters of the subsurface to image the base of sediment fill, even in areas of high sediment accumulation.

For the present study, the sound source was suspended over the side of the coring boat, adjacent to the coring gantry (Figure 2-1). Short acoustic records were collected at each core site while still at anchor. Then complete profiles were collected through each core location. Both the core location and the positioning during profiling were determined using the sub-meter DGPS

system contained within the SDI profiler. During post survey processing of the acoustic data the core locations and depths to the pre-impoundment surface were read into the acoustic processing program. The program posts core diagrams that show the interpreted post-impoundment sediment thickness on the acoustic data at the point of closest approach of the profile to the core location.



Figure 2-8. SDI acoustic profiler control module. (a) The module contains all acoustic profiling and DGPS navigation electronics.

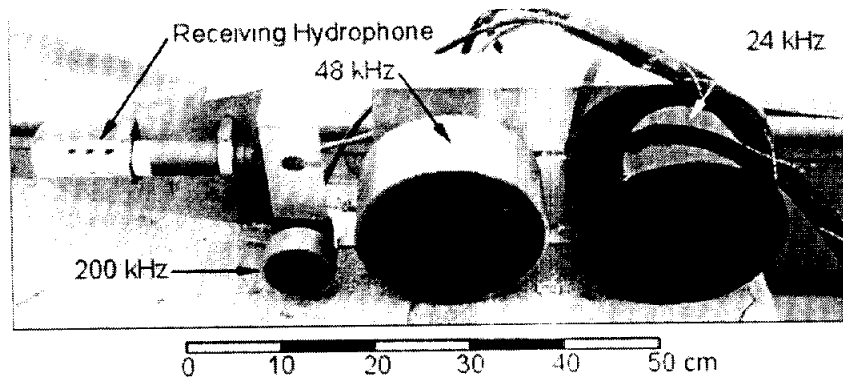


Figure 2-9. Transducer array for SDI acoustic profiler. The system collects acoustic data at 200, 48, and 24 kHz simultaneously along the profile.

3. Results

The watersheds of the four reservoirs considered in this project (Lakes Aquilla, Granger, Limestone, and Proctor) span a range of physiographic provinces, land use, and sediment generating capacities. As a result, the reservoirs are expected to show different sedimentation characteristics. Important watershed sedimentation parameters for the four reservoirs are summarized in Table 3-1. All four reservoirs are formed by rolled earthfill dams. The lakes range in age from 40 years (Lake Proctor) to nearly 20 years (Lake Aquilla). In this project we collected a total of 35 cores from 23 separate locations within the four reservoirs. The total length of core was approximately 31 m. The pre-impoundment surface was reached and sampled at 22 of the 23 sites cored. At locations where significant thicknesses of sediment were found, duplicate cores were collected for analysis by personnel at Texas A&M, Galveston. A summary of core locations, core lengths, and the interpreted depth to the pre-impoundment surface are given in Table 3-2. Tables describing the results of the physical analysis of cores from each site are given in Appendix A.

Table 3-1. Sedimentation characteristics of the four reservoirs considered in this study.

Reservoir	Physiographic Province	Basin Land Use (Averages for Province)	Average Soil Loss Tons/Ac.
Aquilla	Black Land Prairie/East Cross	Farmland/Pasture and Rangeland	2.61/2.06

Granger	Black Land Prairie	Farmland (32% crops and 54% range and pasture)	2.61
Limestone	Texas Claypan/Texas Black Land Prairie	Pasture and Rangeland/Farmland	2.14/2.61
Proctor	Timbers West Cross Timbers	Native grass pastures; rangeland	2.52

Source: Greiner, J.H. (1982) Erosion and Sedimentation by Water in Texas. Texas Department of Water Resources, Rept. 268, Austin, Texas, 145p.

Table 3-2. Summary of sediment cores collected in lakes Aquilla (A), Granger (G), Limestone (L) and Proctor (P). For each core the locations are given in Texas State Plane, North Central (NC) or Central (C) zones, NAD 83. The length of core is given and depth to the pre-impoundment surface is given, if it was reached. Duplicate cores at the same site are designated with lower case letters (a,b,c). Lengths and depths correspond to the core analyzed at that location, indicated with a bold lower case letter for duplicate cores.

Core ID	Easting (ft)	Northing (ft)	Length (cm)	Depth to pre-impoundment (cm)	Texas Zone
A1	2375689.1	6659146.2	16	5	NC
A2a,b,c	2375526.2	6659265.5	305	40	
A3a,b	2368970.8	6656269.5	57	40	
A4	2366880.1	6656075.4	19	4	
A5a,b	2373254.9	6656222.8	77	50	
A6	2369992.4	6651144.9	57	55	
G1a,b	3238346.9	10231787.7	31	29	C
G2a,b	3237701.8	10229734.2	97	83	
G3	3232633.7	10229813.6	205	0	
G4	3232953.6	10230844.4	25	20	
G5	3231636.8	10226956.9	45	36	
G6	3232316.8	10225391.5	225	60	
L1a,b	3551080.5	10469616.8	101	90	C
L2a,b	3537074.0	10502583.0	17	9	
L3a,b	3543238.2	10493981.0	173	40	
L4a,b	3544283.0	10494518.0	5.5	0	
L5	3547248.0	10469649.0	109	100	
P1a,b	2860457.5	10687885.0	46	30	C
P2	2866969.0	10686350.0	13	?	
P3a,b	2866920.9	10685617.7	67	54	
P5	2873250.8	10691241.1	20	4	
P6	2873266.6	10691318.5	265	85	
P7	2874037.2	10691140.1	70	50	

3.1 Lake Aquilla

Impoundment of Lake Aquilla began April 29, 1983. The drainage area supplying the reservoir is 252 square miles. As of 1998, maximum contents was 119,000 acre-feet on December 23, 1991, (elevation 551.89). The minimum contents was 4600 acre-feet, observed on October 6-10, 1983 (elevation 511.31 ft.). Lake Aquilla was last surveyed by the Texas Water Development Board in October, 1995. The previous survey was in 1983. The computed difference in lake volume between the two surveys was -12.3%. For the present study a total of 10 cores were collected in Lake Aquilla at 6 locations (Figure 3-1). The pre-impoundment surface was reached and sampled at each site. At one site (Site A2) the entire thickness of pre-impoundment fluvial deposits was penetrated. Core sites A1 and A4 are located in areas on the

submerged floodplain and show relatively thin sediment deposition (5 – 9 cm). In these submerged floodplain cores the reservoir sediment is silty-clay of high water content (60 to 80% water content) and low shear strength (0.01 to 0.04 kg/cm²). The post-impoundment sediment contained no intact plant material. The pre-impoundment material is highly compacted (25-30% water content), medium shear strength (0.4-1 kg/cm²) silty-clay soil containing intact plant roots. Sites A2 and A5 and are located along the submerged channel of Hackberry Creek. Core A2c reached the interpreted pre-impoundment surface at 40 cm. The reservoir fill is a high water content (60 to 80%) organic-rich, silty-clay, low-density mud. The pre-impoundment material is a lower water content (40 to 60%), higher strength (0.05 to 0.7 kg/cm²) sediment we interpret as a pre-impoundment fluvial deposit within the channel. The base of the cored pre-impoundment is a highly compacted (21% water content), stiff (2 kg/cm²) mixture of silty-clay, gravel and rock fragments. We interpret this surface as the rock channel that pre-dates the most recent stream aggradation. Core A5 was collected on the steep bank of the submerged channel of Hackberry Creek. At Site A5 the pre-impoundment material is tan to dark brown and contains grass roots, like that found in the submerged floodplain cores. Site A3 is located on the submerged channel of Aquilla Creek. It contained 40 cm of similar post-impoundment sediment and a pre-impoundment surface similar to that found at Site A5.

Core descriptions, short acoustic records from the core sites, and physical properties of the core material for core sites A2 and A3 are shown in Figures 3-2 and 3-3. At Core Site 2, the upper 40 cm of the core is composed of low-density mud with water content that ranges from nearly 80% at the water bottom to 60% 40 cm below the bottom. We interpret this layer as the post-impoundment lake sediment. In this case we make the distinction between the pre- and post-impoundment deposits within the channel based on the contrast in water content between the two layers. The texture of the lake sediments is only slightly more clay rich (93.4 % clay on average) than the river deposits (90.8% clay on average). Deposits throughout the core contain almost no sand and range between 5 and 20% silt and the rest clay. Acoustically, this interval is a distinct layer, defined by strong returns at 200 kHz, but relatively low amplitude returns at 48 and 24 kHz. The pre-impoundment fluvial deposits at Site A2 extend to the deepest returns of the 24 kHz signal at 3 m (acoustic basement).

The acoustic response of the reservoir fill is essentially the same at Site A6 (Figure 3-4). At this site the post-impoundment layer of low-density mud is 55 cm thick. The top of the low-density mud layer is marked by a reflection of 48 kHz signal. Continuous returns from the post-impoundment interval occur only at 200 kHz. Most of the post-impoundment interval is transparent to 48 and 24 kHz signals. The pre-impoundment surface is marked by strong reflections at all three signal frequencies and all three signals penetrate a significant distance into the pre-impoundment material. We interpret this material as alluvium deposited at the confluence of Aquilla and Hackberry Creeks.

Acoustic profiles collected through the core sites place the sediment thicknesses observed in the cores in the perspective of how the sediment thickness varies spatially (Figures 3-4, 3-5, 3-6, and 3-7). A striking feature of the Aquilla cores is the contrast between the thin post-impoundment fill layer found on the submerged floodplains (e.g. 5 cm at Core Site A1) on the submerged floodplain and the greater thickness in the submerged channels (e.g. 40 cm at Core Site 2), only 200 ft away. The contrast occurs because Site A1 is located on a local high in the pre-impoundment surface (Figure 3-4). Two distinct acoustic intervals are seen on the profile through Core Sites A1 and A2. The upper interval is nearly acoustically transparent, appearing light gray on the 48 kHz section. This interval corresponds to low-density mud with 60 to 80%

water content that ranges in thickness from 5 to 50 cm along the profile. This low-density mud layer can be traced continuously across the profile, as it thickens in the lows and thins over the highs. We interpret this interval as the post-impoundment deposit. The lower interval produces high amplitude returns at all three signal frequencies and appears dark gray to black or “salt-and-pepper” speckled on the 48 kHz section. We interpret this interval as alluvium deposited by Hackberry Creek prior to impoundment. The alluvium ranges in thickness from 5 cm to over 2.5 m and also thickens in the lows and thins over the highs in the underlying ancestral valley floor.

The profile through Core sites A3 and A4 crosses the Aquilla Creek arm of the reservoir, midway towards the backwater region from the dam. Along this profile only a thin dusting (4 cm at Core Site A4) of post-impoundment sediment has accumulated on the floodplain in 20 years. Much more sedimentation (40 cm at Core Site A5) is focused along the submerged channel of Aquilla Creek. In contrast, along the profile through Site A6, which is close to the dam, the post-impoundment layer is 60 cm thick or more and extends over both on the submerged floodplain and channel. As elsewhere in the lake, the post-impoundment interval is a low-density mud layer that appears light gray on the 48 kHz section (Figure 3-7). The acoustic signals penetrate up to 2 m of pre-impoundment material, which has a relatively flat upper surface and fills deep depressions in the ancestral valley floor. On the profile diagram, Core A6 is represented by a yellow interval corresponding to the 55 cm thickness of post-impoundment sediment over a green interval representing stiff, black clay containing intact plant roots, interpreted to be a pre-impoundment soil formed on alluvium.

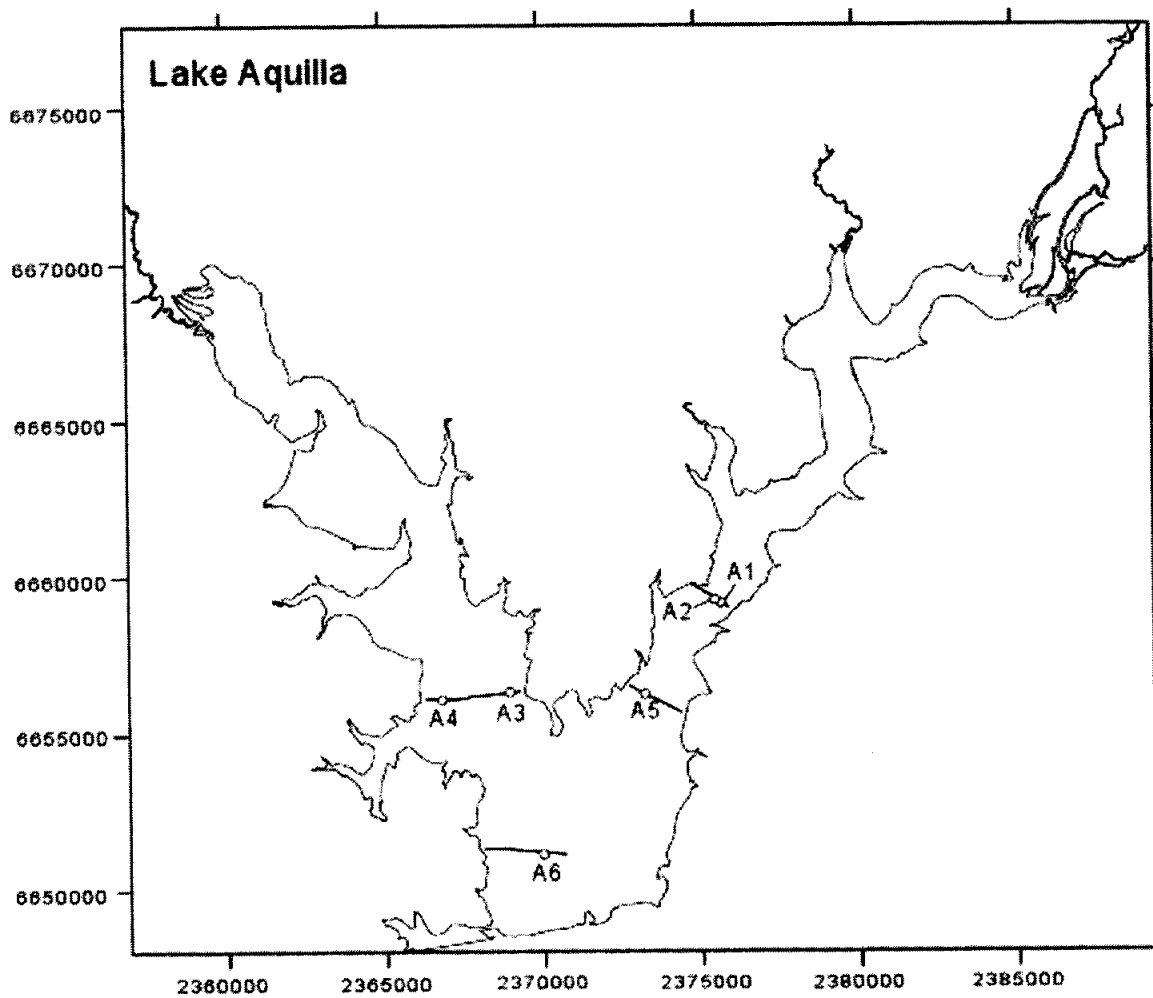


Figure 3-1. Map showing core locations in Lake Aquilla (circles) and the track lines of acoustic profiles collected through the core locations (curves). Map coordinates are Texas State Plane, North Central Zone, NAD 83, feet.

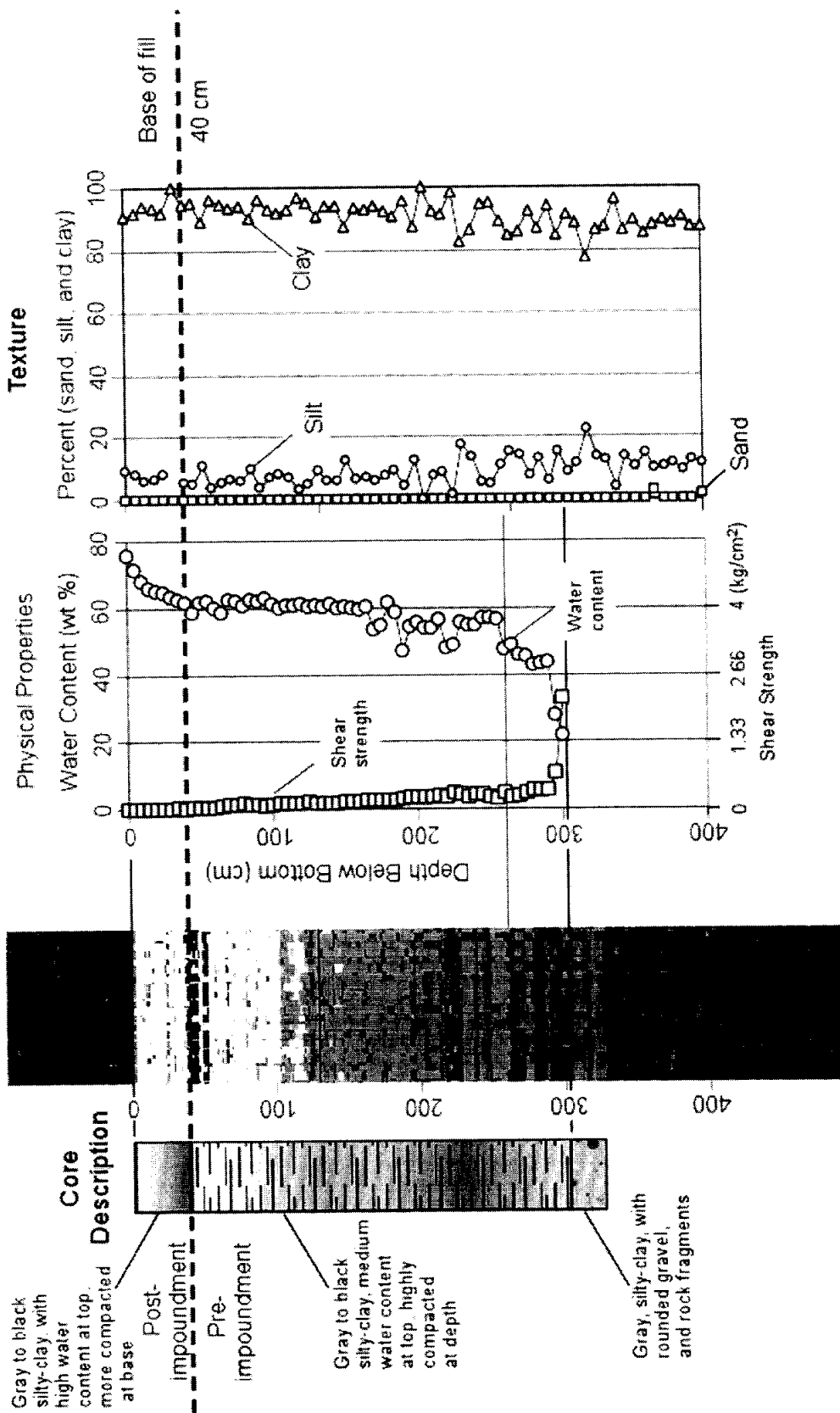


Figure 3-2. Correlation of Aquilla Core A2c and co-located acoustic record. The acoustic record is converted from travel time to depth below the water bottom assuming a speed of sound of 1440 m/s. The location of Core Site A2 is shown in Figure 3-1.

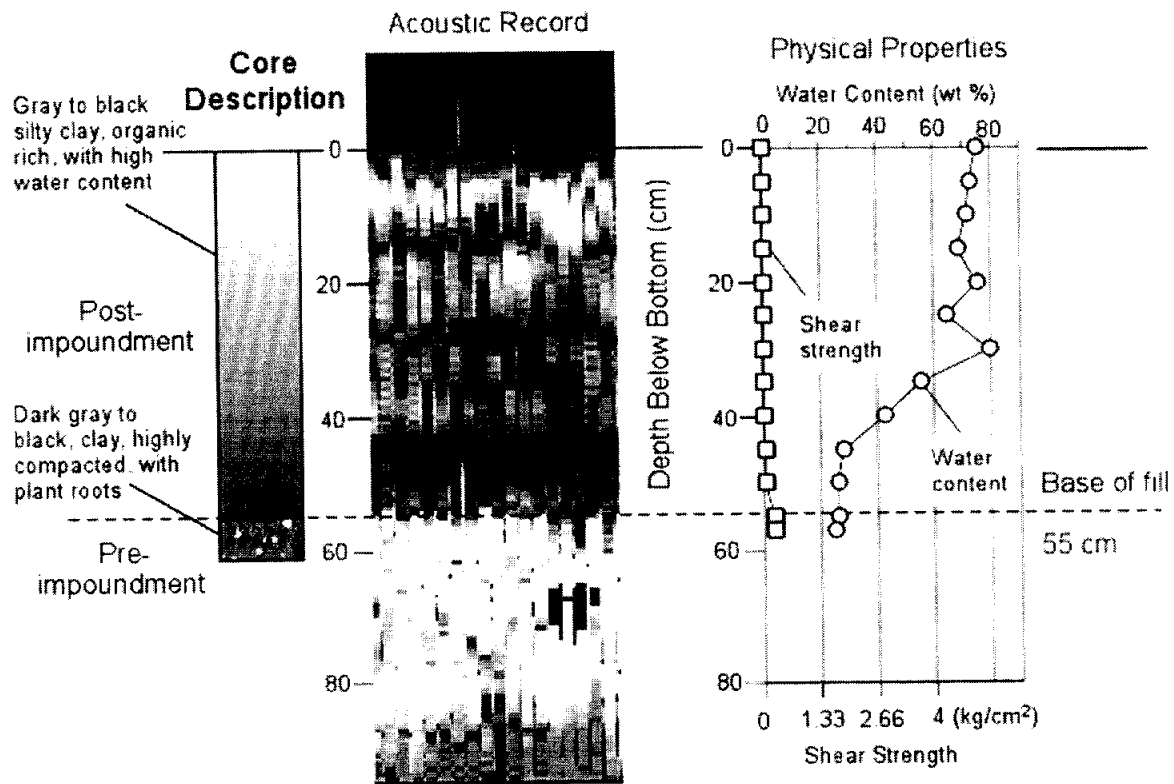


Figure 3-3. Correlation of Lake Aquilla Core A6 and co-located acoustic record. The acoustic record is converted from travel time to depth below the water bottom assuming a speed of sound in sediment of 1440 m/s. The location of Core Site A6 is shown in Figure 3-1.

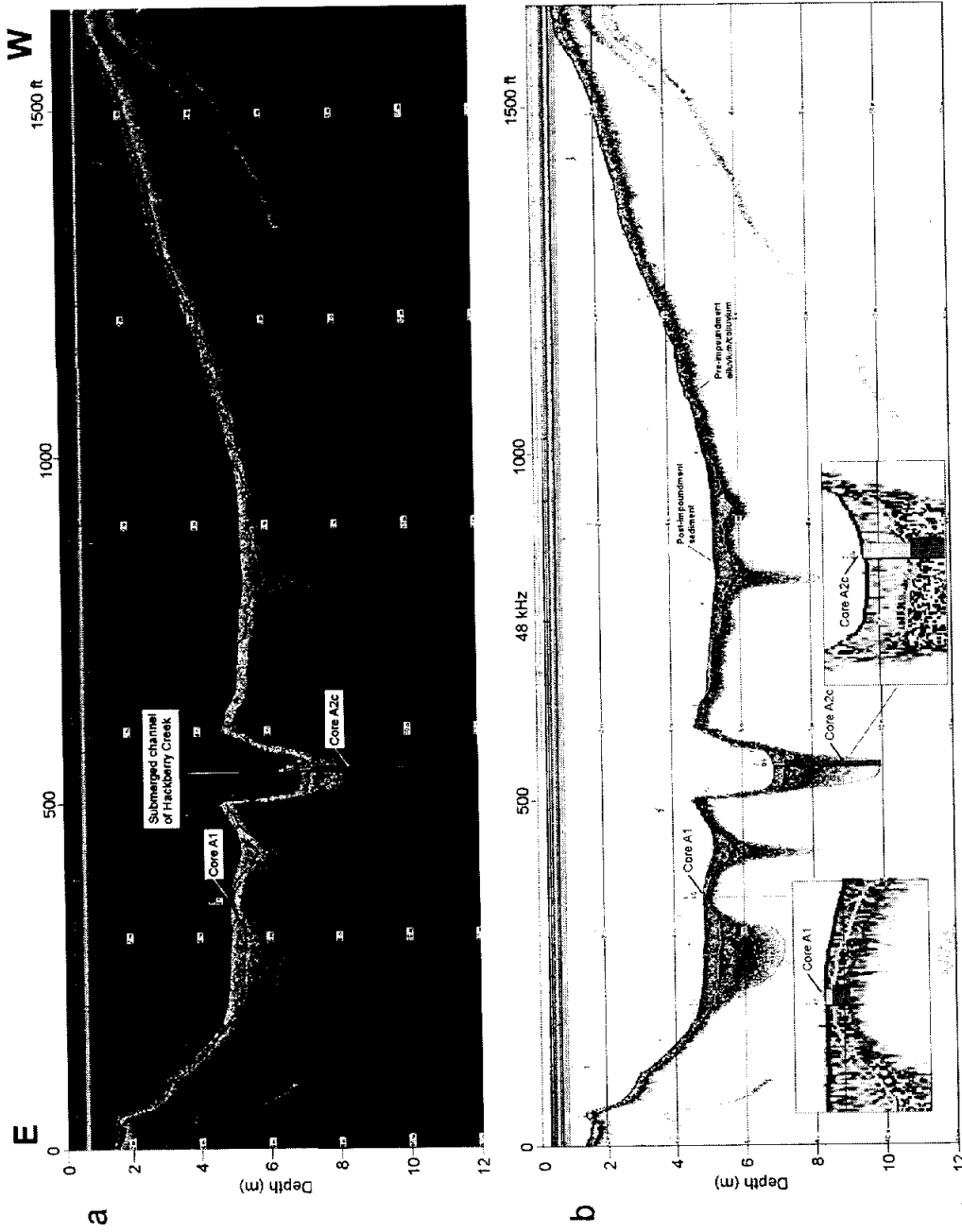


Figure 3-4. Profile through Lake Aquilla Core sites A1 and A2. (a) Composite color display of 200 (red), 48 (green) and 24 kHz (blue). (b) Display of 48 kHz data alone. Core Site A1 is located 4.5 ft from the profile and Core Site A2 is located 0.6 ft from the line. Two intervals are traced on the profile. The upper interval (red-yellow) corresponds to the low-density fluid-mud post-impoundment interval in the cores. The lower interval corresponds to more compacted pre-impoundment alluvium/sediment. In the core diagrams yellow represents post-impoundment fill and green represents pre-impoundment material.

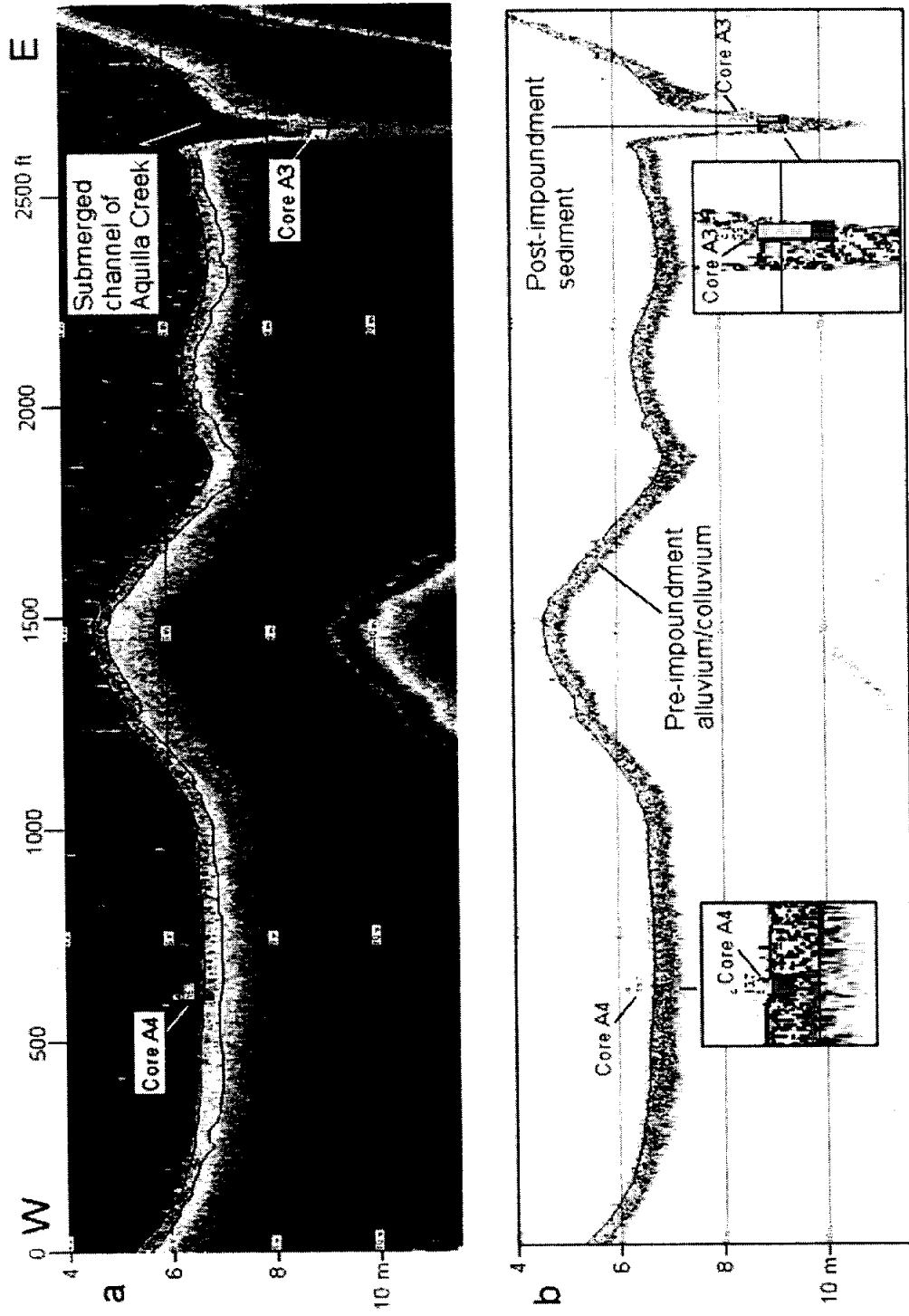


Figure 3-5. Profile through Lake Aquilla Core sites A3 and A4. (a) Composite color display of 200 (red), 48 (green) and 24 kHz (blue). (b) Display of 48 kHz data alone. Only a thin "dusting" (4 cm) of post-impoundment sediment is present over the profile, except within the submerged channel of Aquilla Creek. Core Site A3 is located 23.1 ft from the profile. Core Site A4 is located 15.7 ft from the profile. In the channel the post-impoundment interval (yellow) expands to 40 cm. The pre-impoundment alluvium (green) ranges in thickness from 27 cm over the crest of local highs to 1.6 m in the channel.

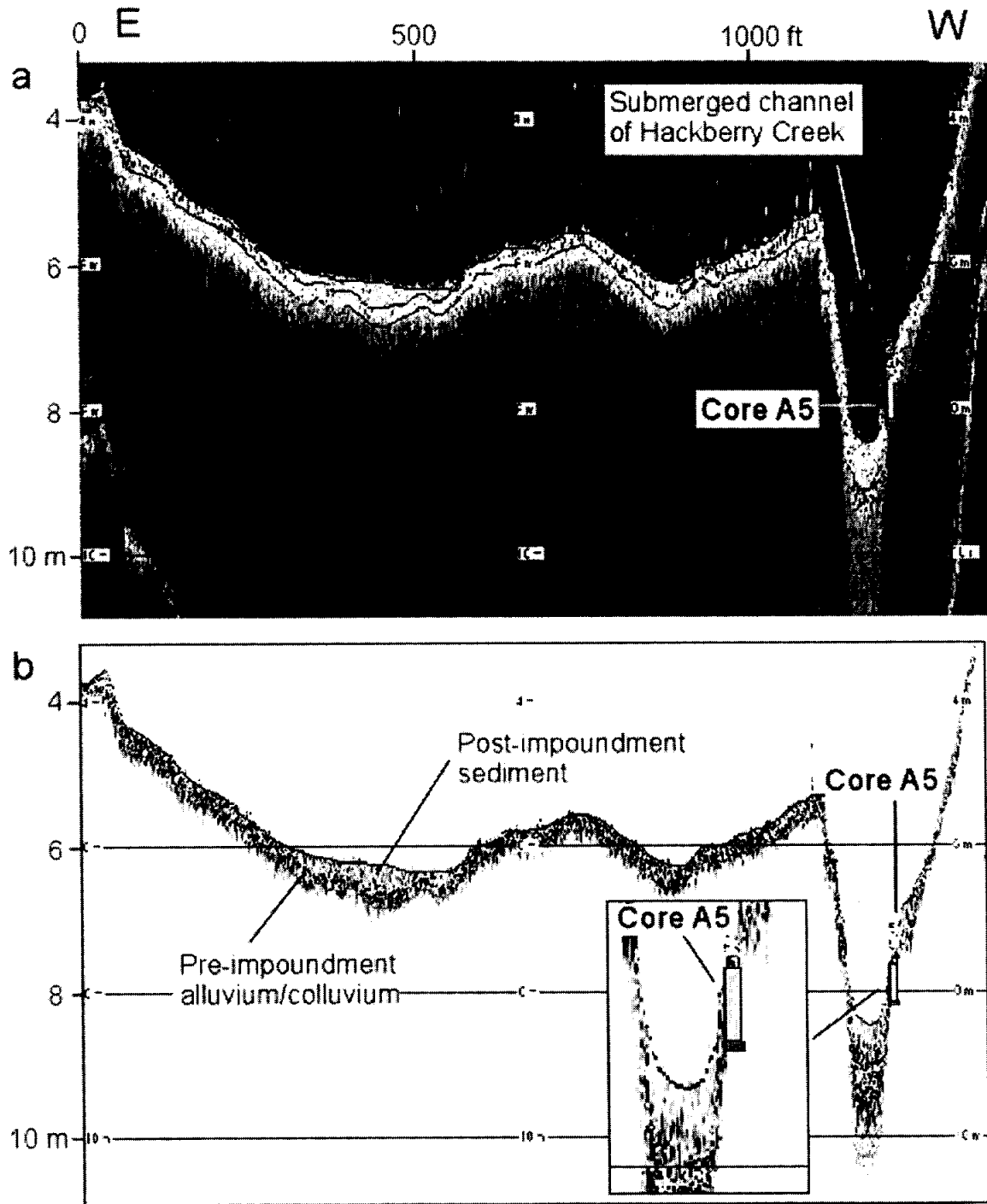


Figure 3-6. Profile through Lake Aquilla Core Site A5. (a) Composite color display of 200 (red), 48 (green) and 24 kHz (blue). (b) Display of 48 kHz data alone. Core Site A5 is located 5.6 ft from the profile. The post-impoundment fill is thickest in the topographic lows in the pre-impoundment surface and pinches out against the topographic highs. In the submerged channel of Hackberry Creek the post-impoundment fill reaches its maximum thickness along the profile of 66 cm. Core A5 missed the axis of the channel and sampled the submerged stream bank, where the post-impoundment sediment (yellow) is 50 cm thick.

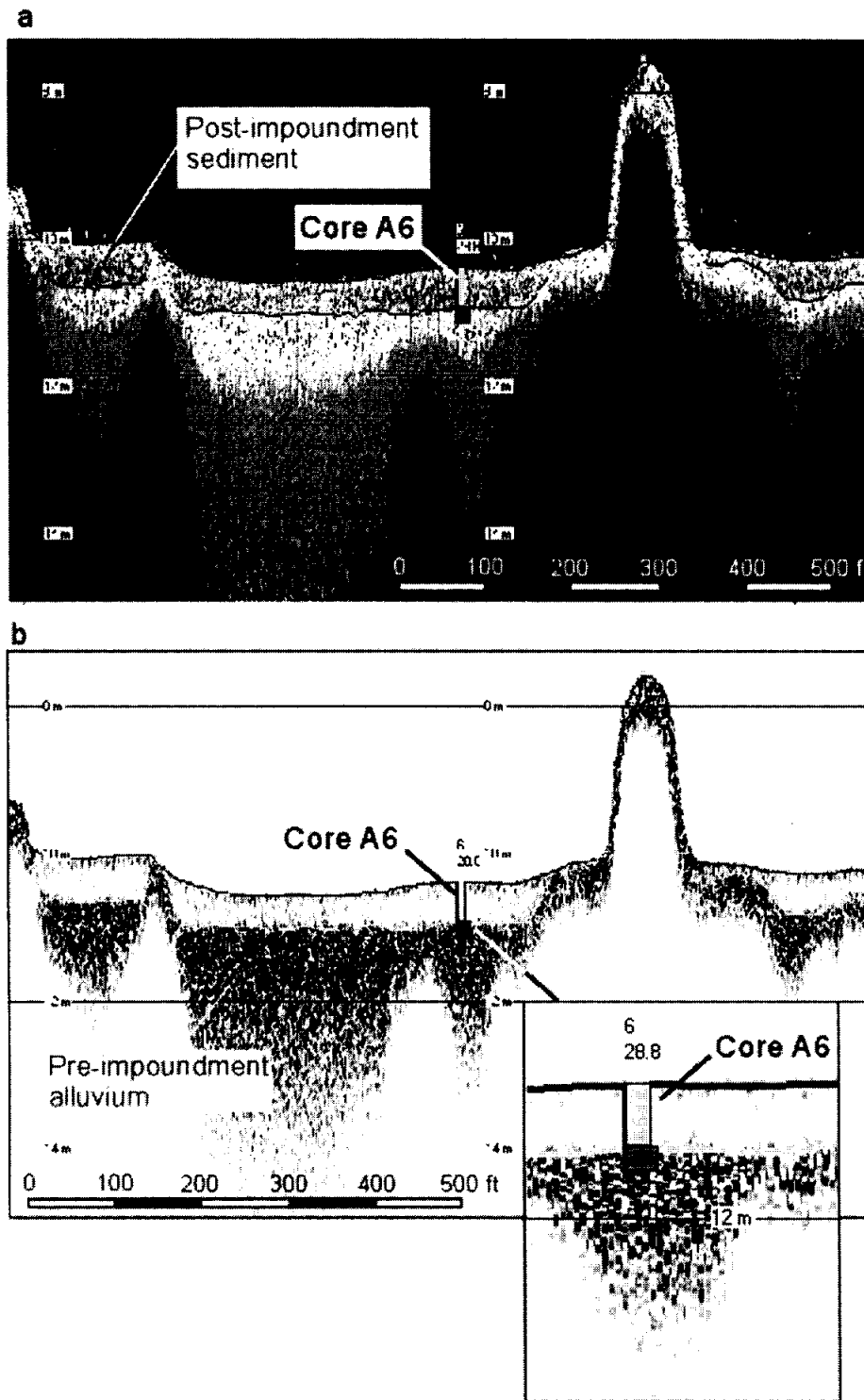


Figure 3-7. Profile through Aquilla Core Site A6. (a) Composite color display of 200 (red), 48 (green) and 24 kHz (blue). (b) Display of 48 kHz data alone. Core Site A6 is located 28.8 ft from the profile. In the core diagrams yellow represents post-impoundment fill and green represents pre-impoundment material.

3.2 Lake Granger

Impoundment of Lake Granger began January 21, 1980. The supplying drainage area to Lake Granger is 730 square miles. As of 1998, the maximum storage was 268,200 acre-feet on March 5, 1992, (elevation 509.22 feet). A minimum storage of 615 acre-feet occurred on January 21, 1980, (elevation 502.80) during the initial filling stage. Lake Granger was last surveyed by the Texas Water Development Board in October 1995. The previous survey, done in 1980, recorded a difference in lake volume between the two surveys of -17.1%. In the current study 8 cores were collected in Lake Granger at 6 locations (Figure 3-4). The pre-impoundment surface was reached at all 6 sites. Most of the core sites (G1, G2, G4, and G5) were located on submerged floodplain or adjacent slopes. Each of these sampled only the top most centimeters of the pre-impoundment material, which was a dense soil containing plant roots on the floodplains and sandy colluvium on the slopes. Two core sites (G3 and G6) were in submerged river channels, where more than 2 m of pre-impoundment fluvial material was recovered. The river-deposited sediments differ little in texture from the lake deposits, but are more compacted and have higher shear strength.

In each setting tested, the acoustic response of the post-impoundment sediments of Lake Granger is distinct from that of the underlying pre-impoundment materials. For example, at Core sites G1 and G2 the post-impoundment deposits produce returns at all three signals and appear yellow to near white on the three-color displays. The various layers of the pre-impoundment materials produce returns primarily at 200 kHz and 24 kHz and appear maroon or 24 kHz alone and appear light blue (Figure 3-9 and 3-10). On the continuous profiles the distinction between pre- and post-impoundment deposits is particularly apparent on the 48 kHz data (Figure 3-11, 3-12, and 3-13). The pre-impoundment produces strong returns that appear black and white speckled and the post-impoundment deposits produces weak continuous returns that appear light gray. On these profiles the post-impoundment fill layer can be continuously traced and ranges from zero thickness, where it pinches out on against the side slopes, to 1 m on the submerged floodplain near the dam. In contrast to the sedimentation patterns found in Lake Aquilla, the post-impoundment layer thins in the submerged river channels (Figure 3-13) and in some places is missing in the channels all together in both upstream positions and near the dam (Figures 3-11 and 3-12). It is not clear whether the lack of post-impoundment fill in the channels is due to nondeposition or erosion. In either case, currents flowing down the submerged channels must play a role in keeping them clear of lake sediments.

The geometry of the pre-impoundment alluvium and colluvium deposits are particularly clear in the Lake Granger acoustic data. In Figure 3-11, 2 m or more of alluvium fills local lows and the main channel axis to produce locally flat pre-impoundment surfaces upon which the post-impoundment sediments were deposited. In Figures 3-12 and 3-13, a continuous layer of alluvium and colluvium is seen draping off the flanking slopes of the lake, reaching a local maximum thickness at the base of the slopes, and extending to and nearly filling the adjacent submerged stream channel with pre-impoundment deposits several meters thick.

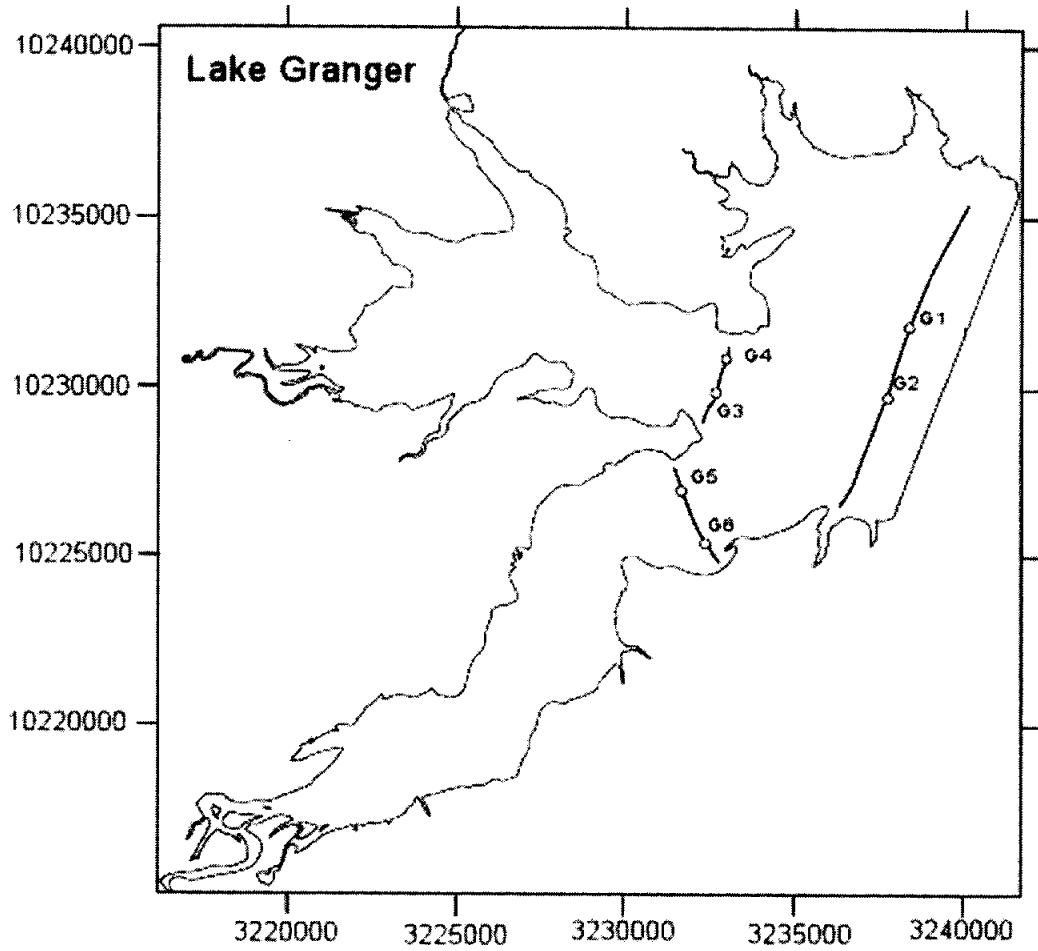


Figure 3-8. Map showing core locations in Lake Granger (circles) and the track lines of acoustic profiles collected through the core locations (curves). Map coordinates are Texas State Plane, Central Zone, NAD 83, feet.

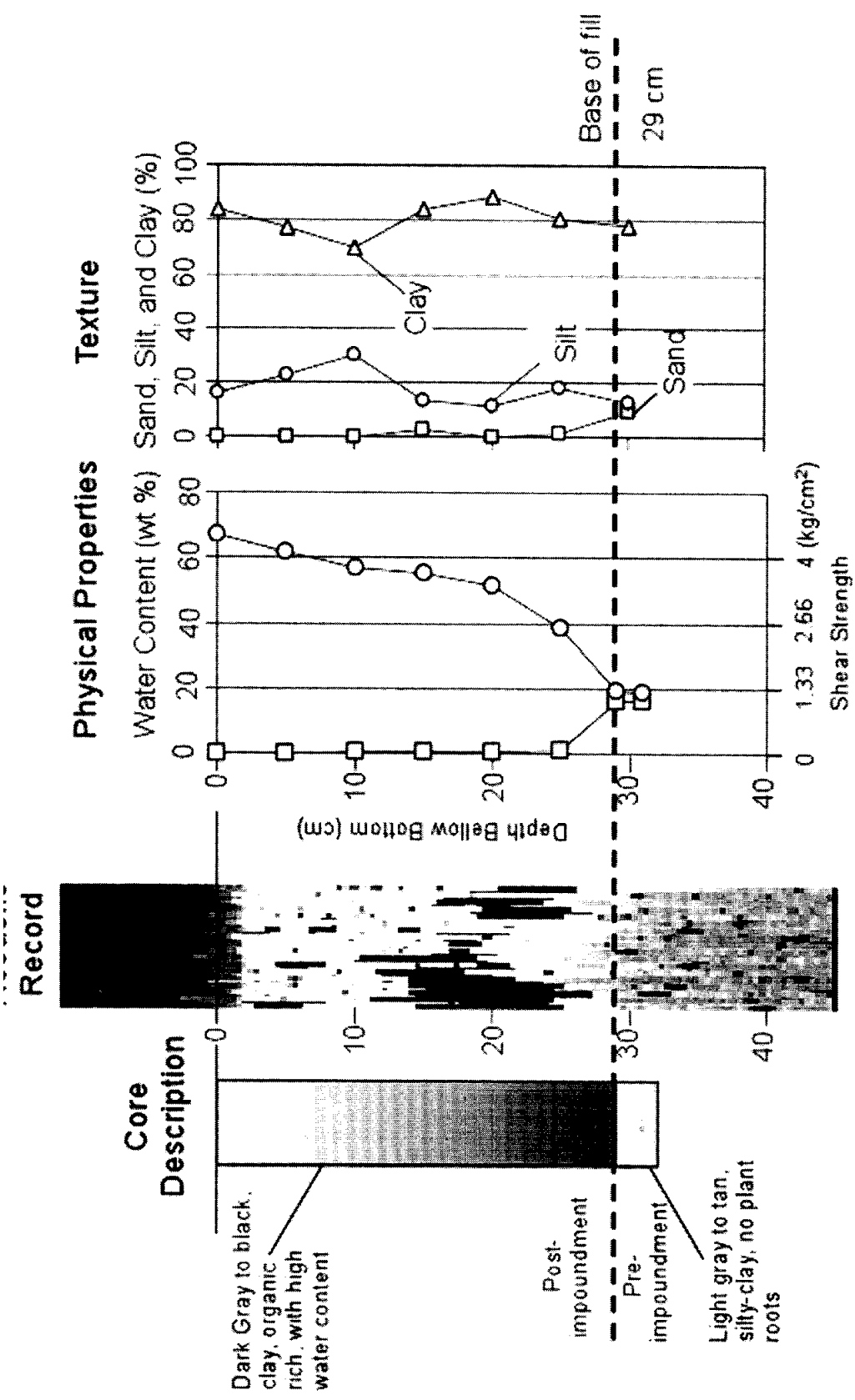


Figure 3-9. Correlation of Lake Granger Core G1a and co-located acoustic record. The acoustic record is converted from travel time to depth below the water bottom assuming a speed of sound of 1440 m/s. The location of Core Site G1 is shown in Figure 3-8.

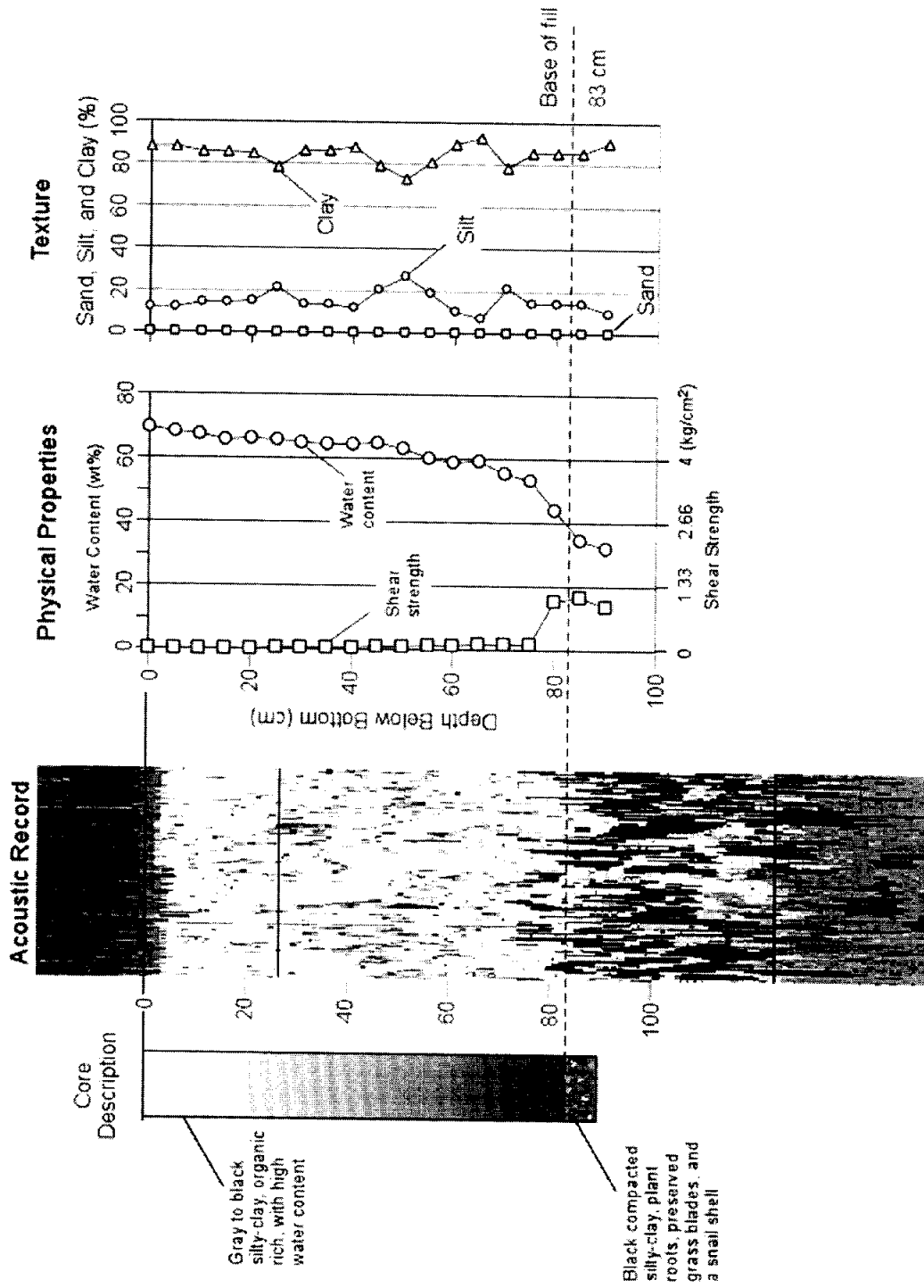


Figure 3-10. Correlation of Lake Granger Core G2a and co-located acoustic record. The acoustic record is converted from travel time to depth below the water bottom assuming a speed of sound in sediment of 1440 m/s. The location of Core Site G2 is shown in Figure 3-8.

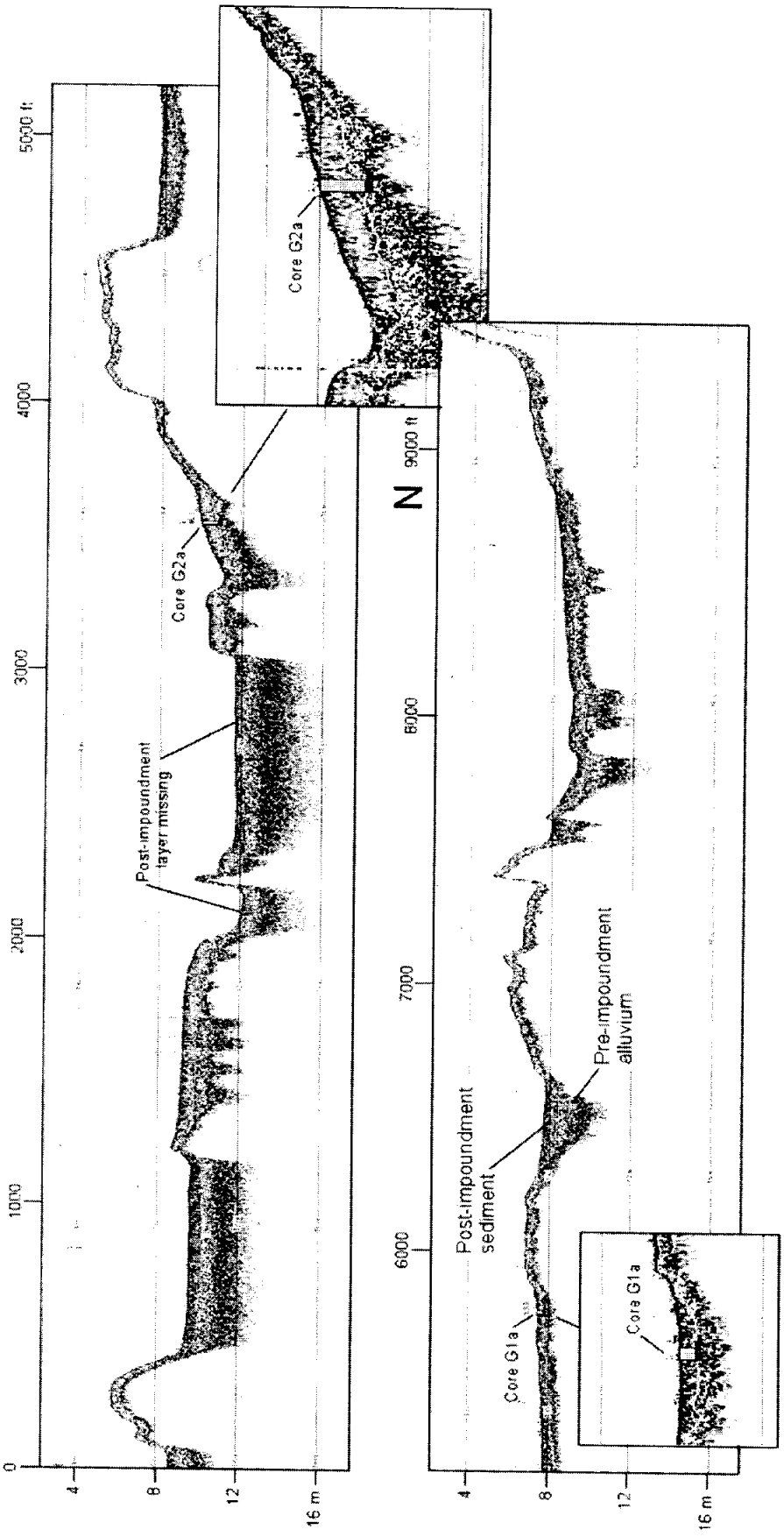


Figure 3-11. Acoustic profile through Lake Granger Core Sites G1 and G2. Core diagrams are shown at the points of closest approach on the 48 kHz profile. The track line of the profile is shown in Figure 3-8. Core Site G1 is located 13.3 ft from the profile. Core Site G2 is located 46.1 ft from the profile. The long profile is shown broken into two segments for display purposes.

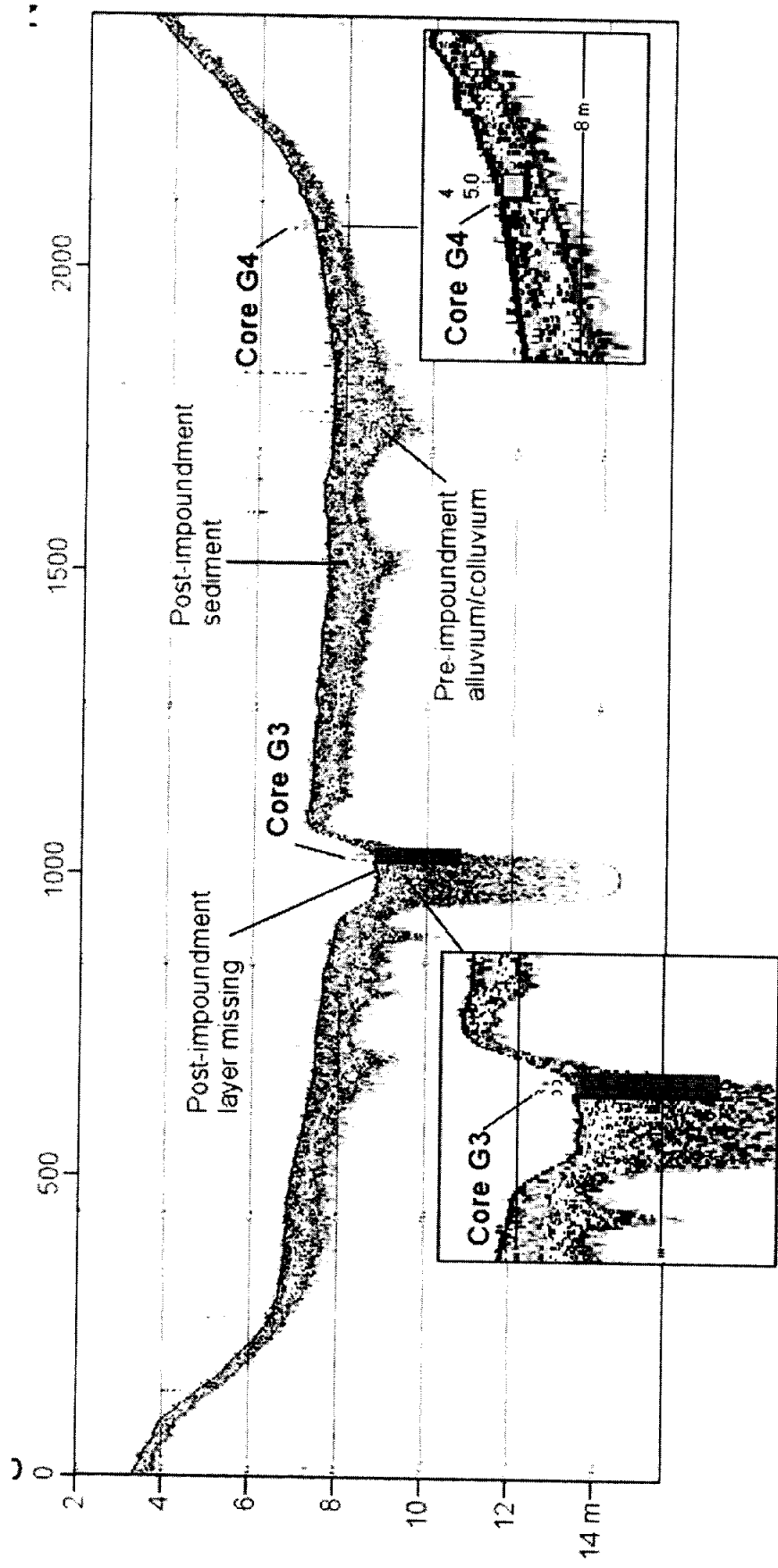


Figure 3-12. Acoustic profile through Lake Granger Core Sites G3 and G4. Core diagrams are shown at the points of closest approach on the 48 kHz profile. Core Site G3 is located 3.3 ft from the profile. Core Site G4 is located 5.0 ft from the profile. The track line of the profile is shown in Figure 3-8.

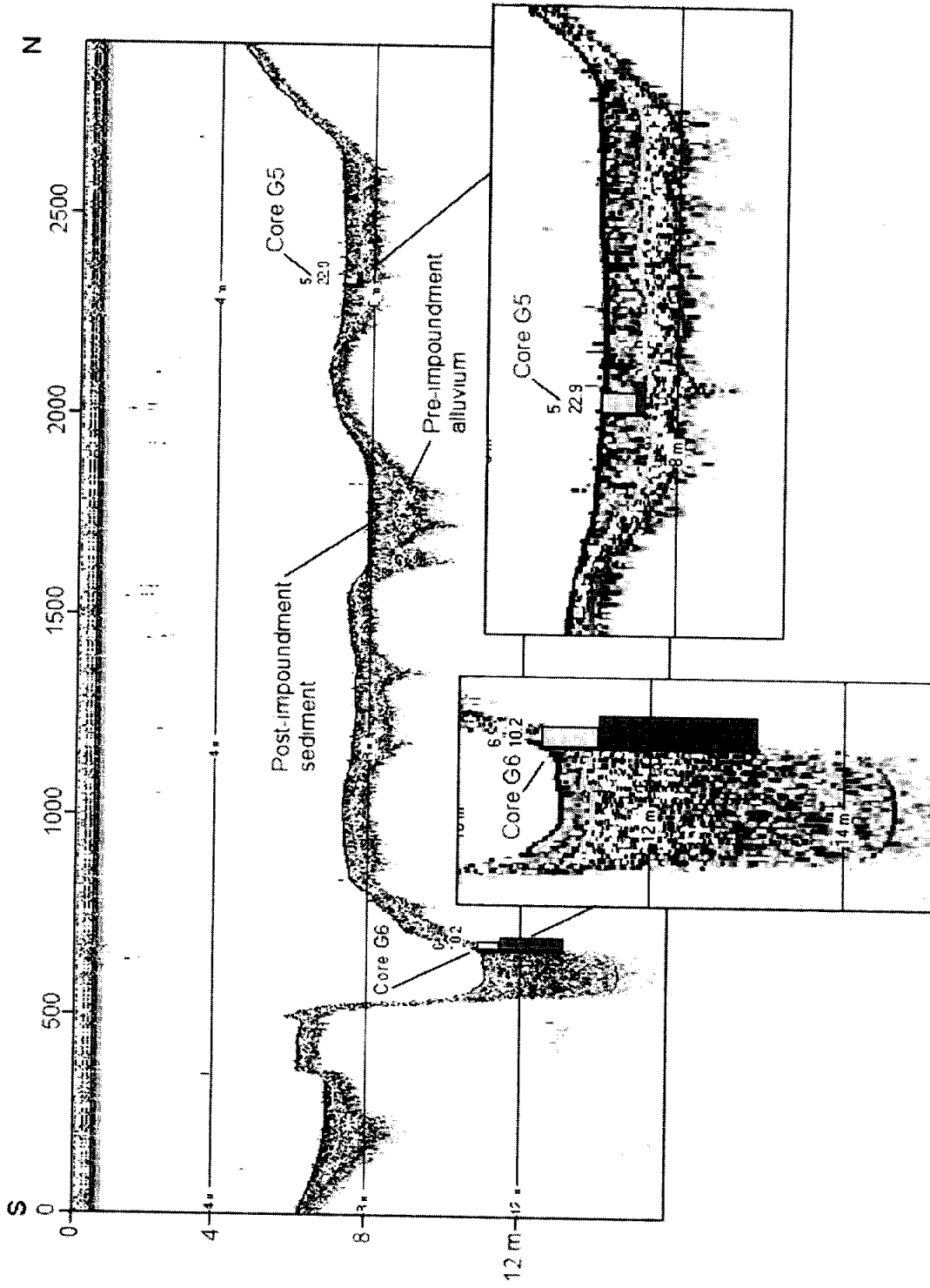


Figure 3-13. Acoustic profile through Lake Granger Core Sites G5 and G6. Core diagrams are shown at the points of closest approach on the 48 kHz profile. Core Site G5 is located 10.2 ft from the profile. Core Site G6 is located 22.9 ft from the profile. The track line of the profile is shown in Figure 3-8.

3.3 Lake Limestone

Lake Limestone is formed by a 11,395 feet long earthfill dam. Impoundment began on Oct. 16, 1978. The drainage area that supplies the reservoir is 675 square miles. In the current project we collected 9 cores in Lake Limestone at 5 locations (Figure 3-14). The pre-impoundment surface was reached and sampled at each site. Core sites L1, L2, L4, and L5 are located in on the submerged floodplain and show a range in sediment deposition (0 – 85 cm). Core site L3 is in the submerged river channel, where 40 cm of post-impoundment sediment overlays an unknown thickness (≥ 133 cm) of pre-impoundment river deposits. In all the cores the post-impoundment sediment is silty-clay with high water content (50 to 80%) and low shear strength (0.01 to 0.04 kg/cm²). The post-impoundment sediment normally contains no intact plant material. One possible exception to these characteristics was found at Core Site L5, located close to the dam. Near the base of this core we found 15 cm of almost pure sand containing one or two small plant roots. We might have interpreted this as the pre-impoundment surface, except that this sandy layer was directly deposited on a 5 cm thick layer of humus containing leaf litter, tree bark, twigs, and intact plant roots. We interpret the top of the humus layer as a forest floor that formed the pre-impoundment surface and the sand layer as material deposited on the forest floor during the construction of the dam or during the early stages of the filling of the reservoir. Throughout the reservoir, the pre-impoundment material is highly compacted (25-30% water content), medium shear strength (0.5-1 kg/cm²) silty-clay soil containing intact plant roots.

Core descriptions, short acoustic records from the core sites, and physical properties of the core material for core sites L1 and L5 are shown in Figures 3-15 and 3-16, respectively. At Core Site L1, the upper 90 cm of the core is composed of low-density mud with water content that ranges from over 80% at the water bottom to 52% 90 cm below the bottom. We interpret this layer as the post-impoundment lake sediment. Acoustically, this interval is a distinct layer, defined by strong returns at all three signal frequencies, but particularly from the 200 kHz signal. This causes the post-impoundment interval to vary from white to yellow, with some purple on the three-color displays. The post-impoundment layer lies directly on a more compact interval with a water content of 35 %, containing pine bark, roots and sand, which we interpret as a pre-impoundment soil interval. Acoustic returns of the 24 kHz signal are the only returns from the pre-impoundment interval, giving it a light blue color on the three-color displays. A similar physical core description and acoustic response is seen at Core Site L5, at the opposite end of the dam (west) from Core Site L1, with the exception of the 15 cm sandy layer, deposited directly on the pre-impoundment surface (Figure 3-16). This sandy interval causes the acoustic response of base of the post-impoundment interval to contain some light and dark blue in the three-color display and to be less distinct than seen at Core Site L1.

Acoustic profiles collected through the core sites show that the post-impoundment fill is easily traced as a white and purple speckled layer over a light and dark blue layer in the three-color acoustic displays (Figure 3-17) or as a light gray layer over a black and white speckled layer on the 48 kHz displays (Figure 3-18). The overall pattern of post-impoundment deposition is similar to that found in Lake Aquilla. In the upstream end of the reservoir the post-impoundment deposits are confined to the submerged river channel. In the middle reaches the post-impoundment deposits are found in local lows in the submerged floodplain as well as in the channel. Near the dam post-impoundment sediments are broadly deposited over both the submerged floodplain and channels in a relatively uniform layer, about 1 m thick.

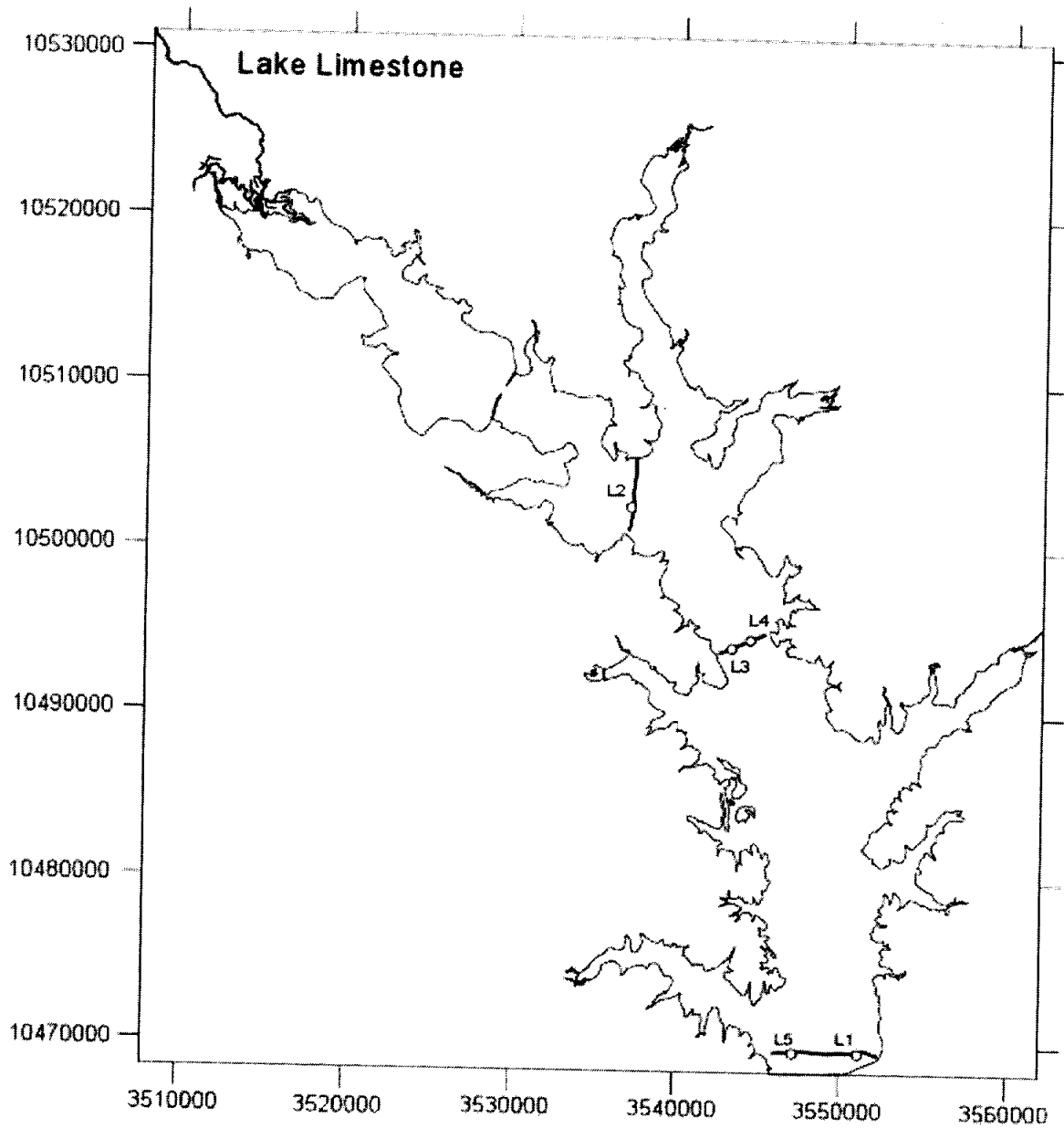


Figure 3-14. Map showing core locations in Lake Limestone (circles) and the track lines of acoustic profiles collected through the core locations (curves). Map coordinates are Texas State Plane, Central Zone, NAD 83, feet.

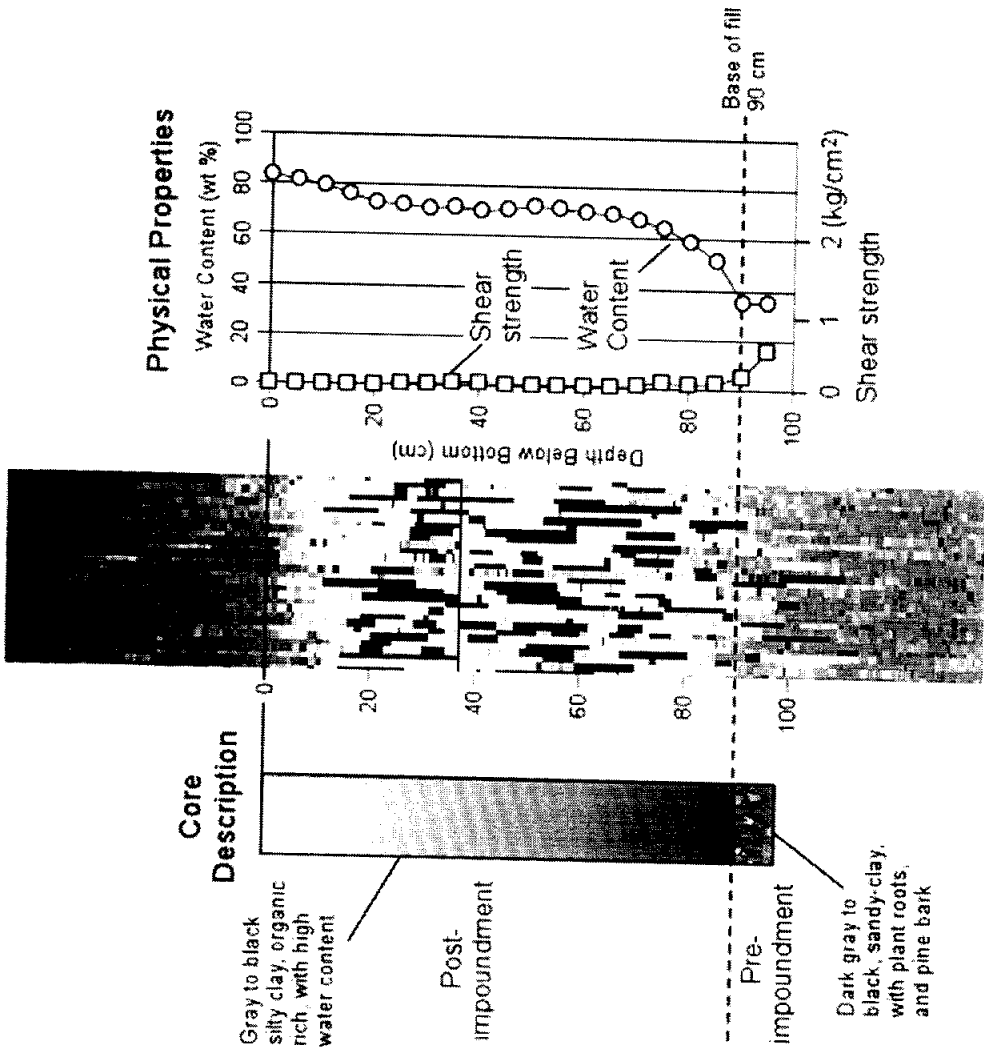


Figure 3-15. Correlation of Lake Limestone Core L1b and co-located acoustic record. The acoustic record is converted from travel time to depth below the water bottom assuming a speed of sound in sediment of 1440 m/s. The location of Core Site L1 is shown in Figure 3-14.

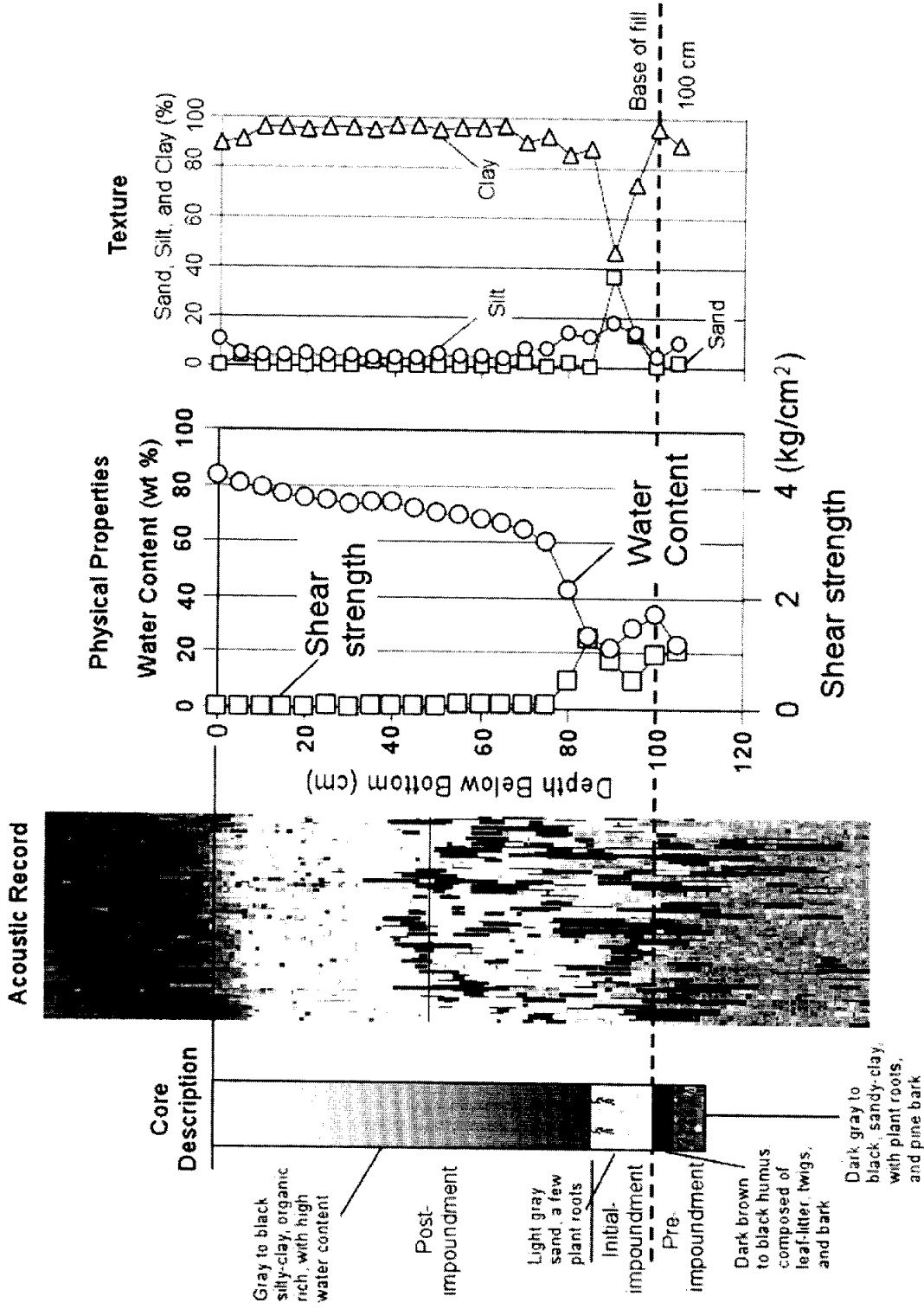


Figure 3-16. Correlation of Lake Limestone Core L5 and co-located acoustic record. The acoustic record is converted from travel time to depth below the water bottom assuming a speed of sound in sediment of 1440 m/s. The location of Core Site L.1 is shown in Figure 3-14.

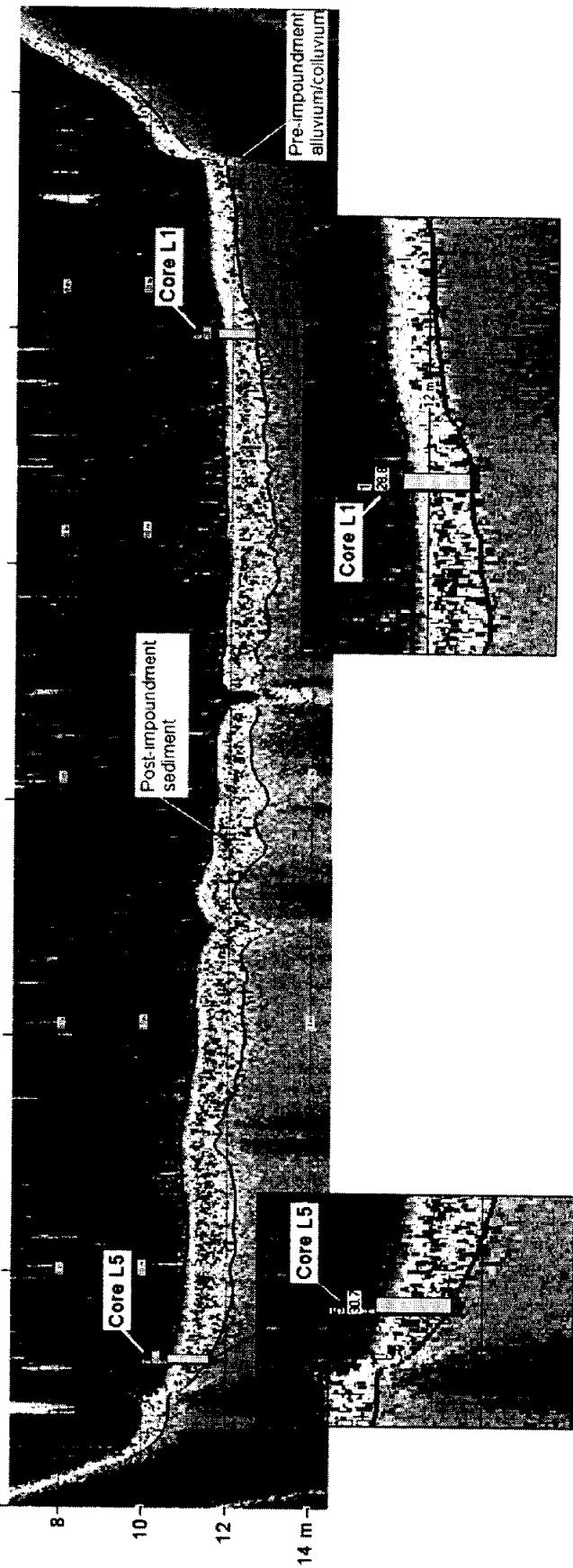


Figure 3-17. Acoustic profile through Lake Limestone Core Sites L1 and L5. The core diagrams show the post-impoundment sediment in yellow and the pre-impoundment material in green. Core Site L5 is located 30.7 ft from the profile. Core Site L1 is located 28.8 ft from the profile. The track line of the profile is shown in Figure 3-14.

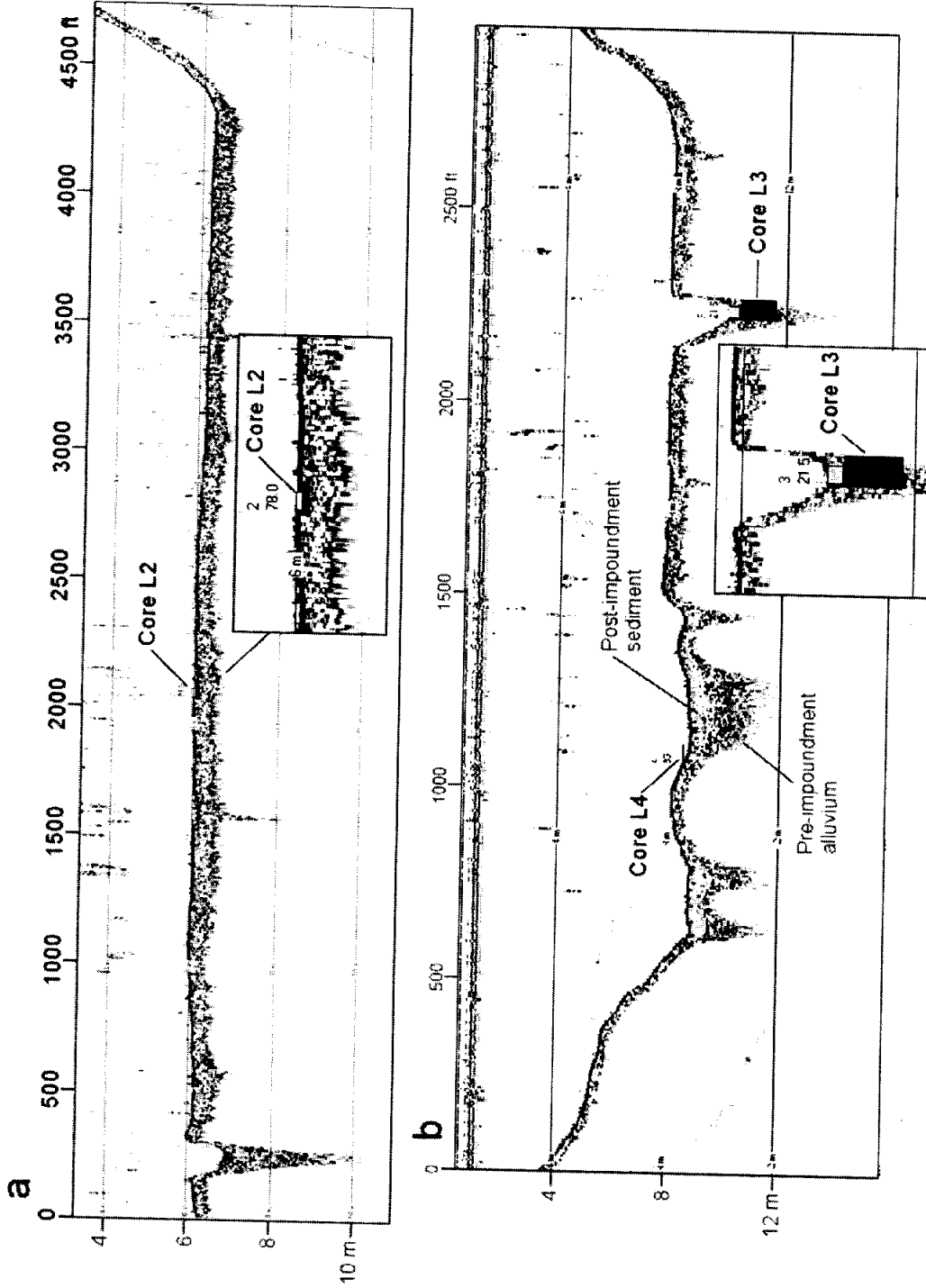


Figure 3-18. Acoustic profiles through Lake Limestone Core Sites L2, L3 and L4. (a) Profile through Core Site L2. (b) Profile through Core sites L3 and L4. Core Sites L2, L3, and L4 are located 78.0, 31.5 and 85.1 ft from the profiles, respectively. Core diagrams are shown at the points of closest approach on the 48 kHz profile. The track line of the profile is shown in Figure 3-14.

3.4 Lake Proctor

Impoundment of Lake Proctor began September 30, 1963. The drainage area supplying the reservoir is 1,265 square miles. As of 1998, the maximum storage was 383,100 acre-feet on May 2, 1990 (elevation, 1,197.63 feet). The minimum storage since the first filling of lake, 18,900 acre-feet occurred on Oct. 4, 1984 (elevation, 1,149.37 ft.). For the present study 8 cores were collected in Lake Proctor at 6 locations (Figure 3-19). Core sites P1, P2, P3, P5, and P7 are on the submerged floodplain. Core site P6 is located in the submerged channel of the Leon River. An initial attempt to core sediments in the submerged Leon River channel (Site P4) penetrated 12 ft of lake and river sediments, but the core was lost during retrieval. The pre-impoundment surface was reached and sampled at each site, except for Core Site P2 and P4.

At Site P1 only 4 cm of high water content, low shear strength sediment overlay highly compacted (31 to 32% water content), high shear strength (1.6 kg/cm^2) sediment of similar color and texture. The compacted sediment was dark gray to black as a result of high organic content, except where it was mottled with light tan vertical streaks. The contacts between the dark gray and tan material were sharp. Further down in the core the water content increased and the shear strength dropped before a second highly compacted layer was reached at depth of 30 cm. The second compacted layer contained many intact plant roots and is interpreted as a soil. Core Site P1 is located in 4.75 ft (15.6 ft) of water. We interpret the first compacted surface to be a desiccation surface formed as the lake sediment dried during a prolonged period of exposure due to low lake levels, perhaps in the mid 1980's. The 4 cm of high water content sediment deposited on top of the desiccation surface is the amount of sediment deposited since that major draw-down event. We interpret the tan mottling within the compacted sediment as washed in material from the banks that filled mud cracks within the dried lake sediment. A similar situation was found at Core Site P2, which is in 7 m (23 ft) of water. However, at this site the vibracore penetrated only 13 cm of sediment before refusal. There was a thin dusting (3 cm) of low-density sediment followed by 10 cm of uniform, compact (30% water content), high shear strength (1.9 kg/cm^2), organic-rich, silty-clay. The recovered sediment looks like post-impoundment sediment recovered elsewhere in the reservoir, except that it is more highly compacted and much higher in shear strength, sufficiently high that it could not be penetrated by the vibracore. As a result, the core did not reach the pre-impoundment surface.

Core descriptions, short acoustic records from the core sites, and physical properties of the core material for core sites P3 and P6 are shown in Figures 3-20 and 3-21. At Core Site P3, the upper 54 cm of the core is composed of low-density mud with water content that ranges from nearly 80% at the water bottom to 60%, 54 cm below the bottom. We interpret this layer as the post-impoundment lake sediment. The underlying pre-impoundment material was also dark gray to black, but was highly compacted (30 % water content) and contained numerous intact plant roots. The pre-impoundment surface is associated with an abrupt drop in water content and an increase in shear strength. The short acoustic record taken at the core site shows high amplitude returns at all three signal frequencies from the post-impoundment sediment layer. As a result, the post-impoundment layer is white to yellow with some red specks on the three-color displays. Only the 24 kHz signal shows significant returns from the pre-impoundment interval, giving it a light to dark blue appearance in the three-color displays. The depth to the pre-impoundment surface at Site P3 based on the core analysis closely correlates to the apparent depth to the pre-impoundment surface based on the short acoustic record collected at the site while still at anchor (Figure 3-20). The correlation is not as good between the coring results and the profile collected

through Site P3, in spite of the fact that the profile passes only 7.1 ft from the core location (Figure 3-23).

At Core Site P6, in the submerged Lean River channel, we made the distinction between the post-impoundment lake deposits and the pre-impoundment river deposits within the channel primarily based on the sharp drop in water content between the two layers (Figure 3-21). Also, the texture of the lake sediment is significantly more clay rich (93.2% clay on average) than the river deposits (86.5% clay on average). The lake sediments contain almost no sand (1.7% on average), whereas the river deposits contain a consistent, small component of sand (5.7% on average). The interpreted post-impoundment layer appears as a distinct interval on the acoustic record, defined by strong returns at all signal frequencies, particularly the 200 kHz. As a result, the post-impoundment interval appears white to yellow, with some areas of red on the three-color displays. The pre-impoundment fluvial deposits at Site P6 extend to the deepest returns of the 24 kHz signal at 1.7 m below the base of the post-impoundment interval (acoustic basement).

On the acoustic profiles through the Lake Proctor core sites, the base of the post-impoundment interval is clear and easily traceable throughout (Figures 3-22, 3-23, and 3-24). The profiles indicate that the overall distribution of post-impoundment sediment in Lake Proctor is different from that found in the other three reservoirs in this study. In Lake Proctor the post-impoundment interval covers both submerged river channels and floodplains near the dam and in the up stream portions of the reservoir. The profiles also show a close correlation between the acoustically based depth to the pre-impoundment surface and the coring results (Figure 3-22 and 3-24), except for core sites P2 (which did not reach the pre-impoundment surface) and P3 (Figure 3-23). Because Core P3a correlates closely with the short acoustic record take at the site, we assume that the miss-correlation between P3a and the profile is caused by variability in the sediment thickness within the 7.1 ft between the core location and the profile. In spite of the apparent desiccation of the lake sediments at sites P1 and P2, the acoustic profiles record the full thickness of the lake sediments. No false base of sediment appears on the acoustic profiles. If the thickness of the post-impoundment interval had been measured by the conventional spud bar penetration method, the measurements would have been significantly less than the true sediment thickness.

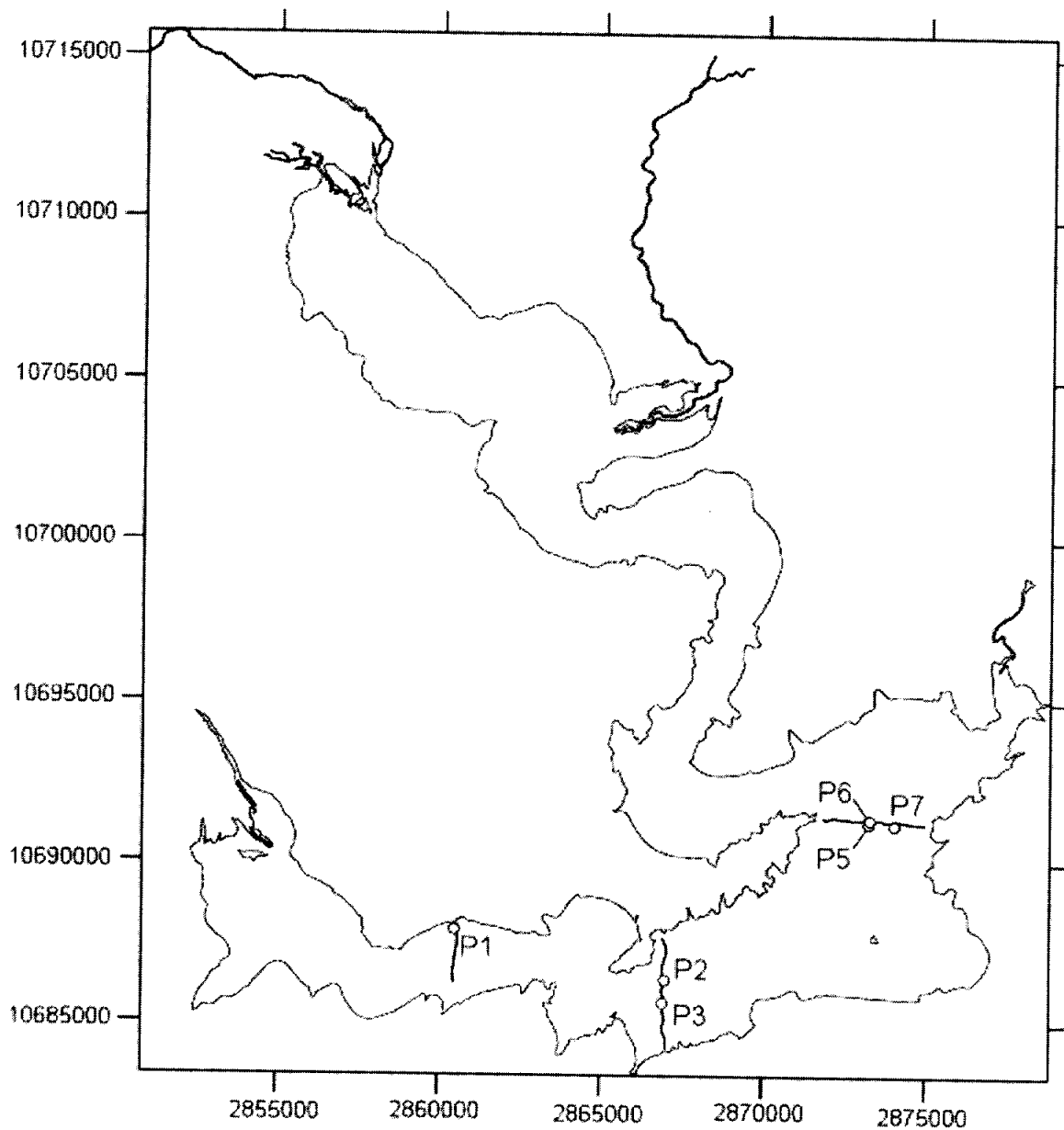


Figure 3-19. Map showing core locations in Lake Proctor (circles) and the track lines of acoustic profiles collected through the core locations (curves). Map coordinates are Texas State Plane, Central Zone, NAD 83, feet.

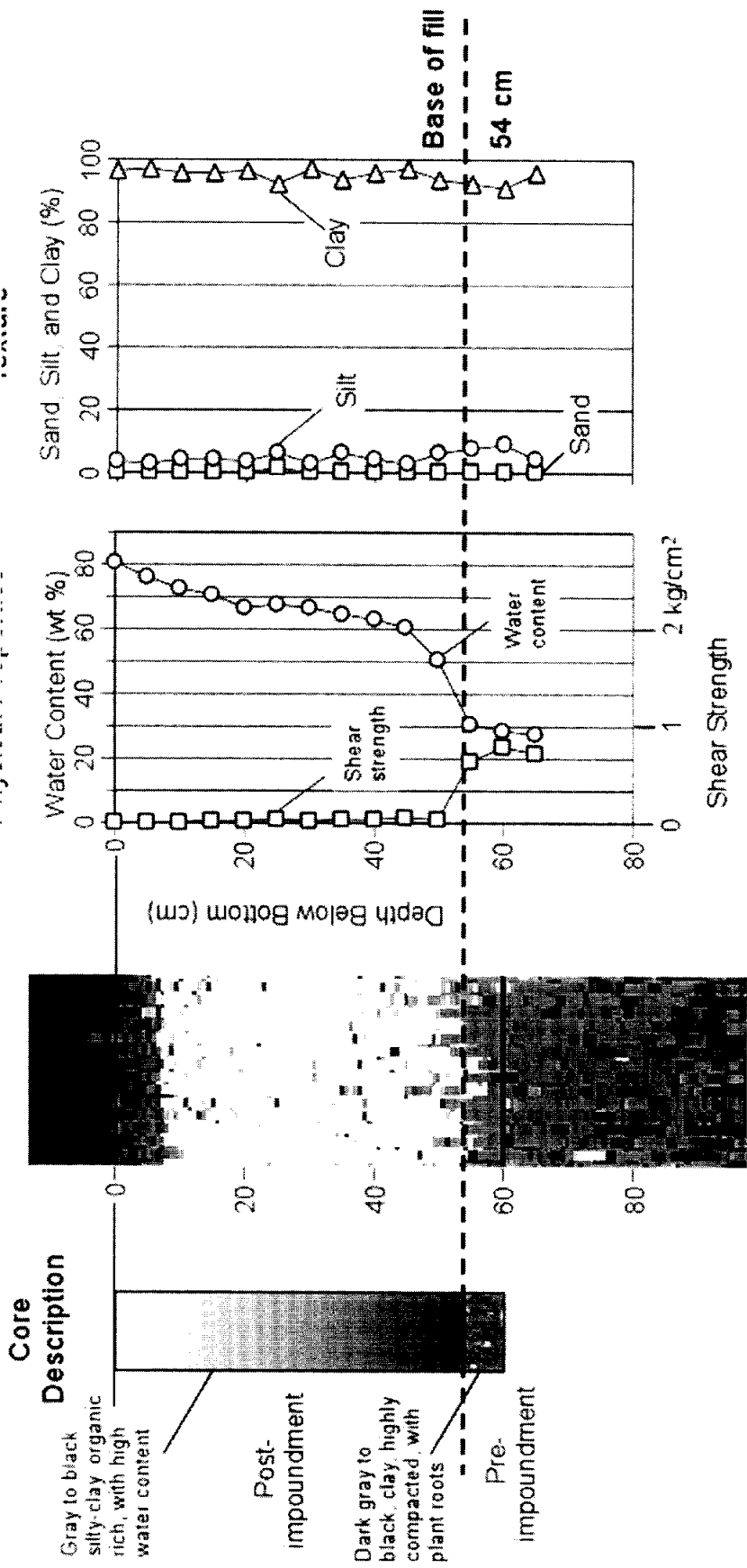


Figure 3-20. Correlation of Lake Proctor Core P3a and co-located acoustic record. The acoustic record is converted from travel time to depth below the water bottom assuming a speed of sound in sediment of 1440 m/s. The location of Core Site P3a is shown in Figure 3-19.

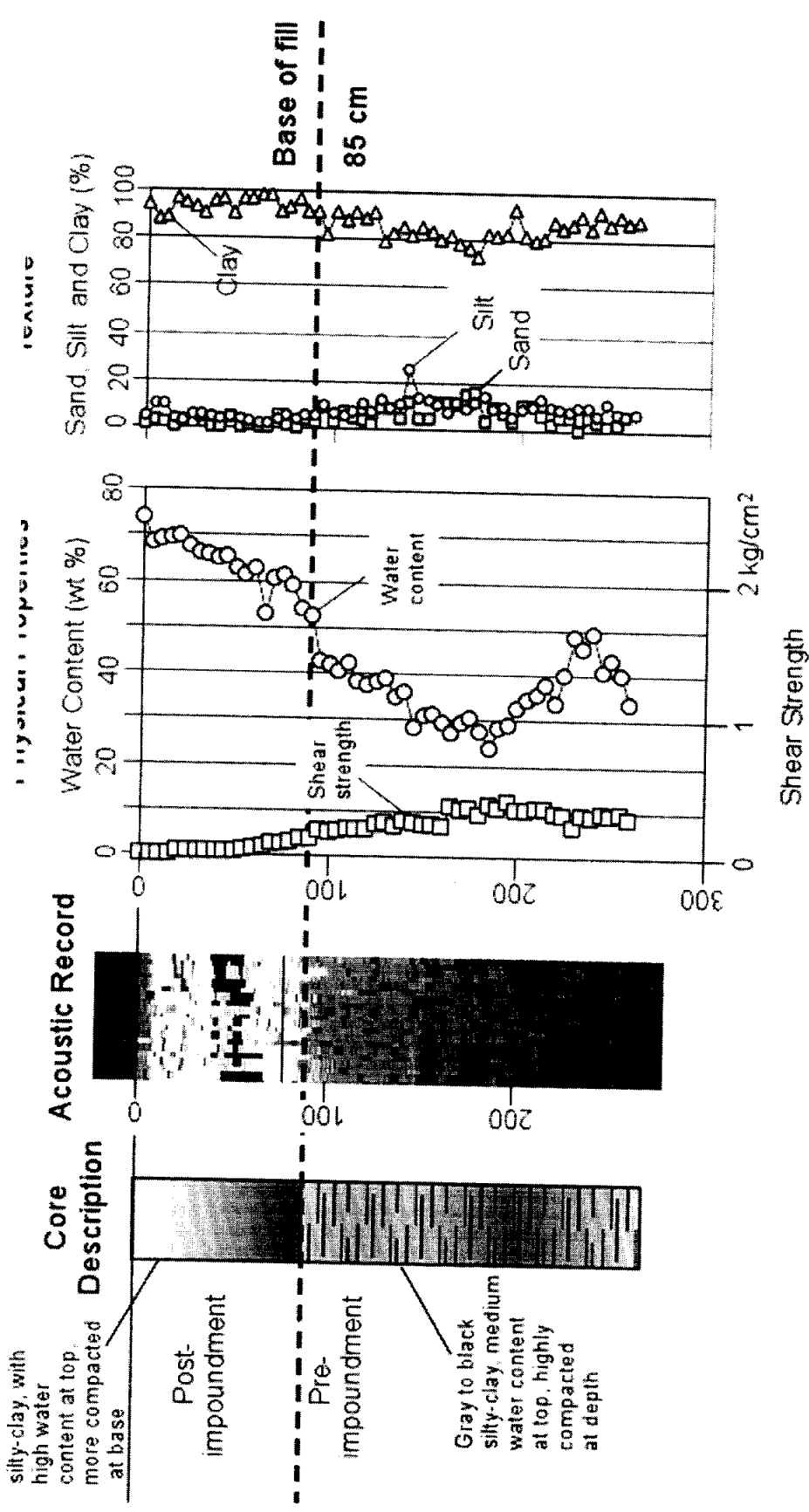


Figure 3-21. Correlation of Lake Proctor Core P6 and co-located acoustic record. The acoustic record is converted from travel time to depth below the water bottom assuming a speed of sound in sediment of 1440 m/s. The post-impoundment sediments have a lower shear strength, higher water content and higher clay content than the underlying river deposits. The location of Core Site P6 is shown in Figure 3-19.

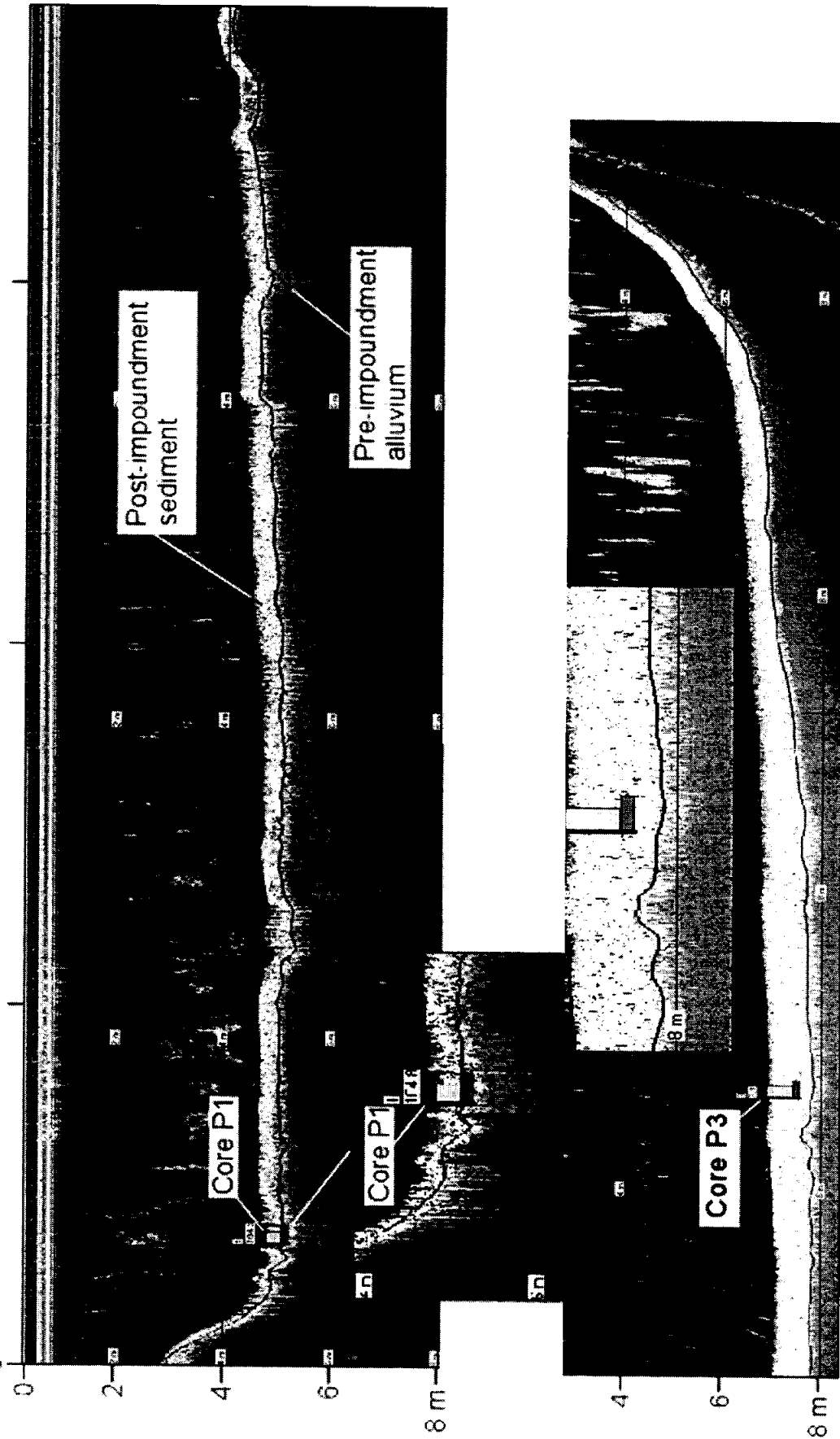


Figure 3-22. Acoustic profile through Lake Proctor Core Site P1. Core diagrams are shown at the points of closest approach on the profile. Core Site P1 is located 104.8 ft from the profile. The track line of the profile is shown in Figure 3-19. The thickness of high-water content post-impoundment sediment observed in Core P1 (30 cm) matches that observed on the acoustic profile.

Figure 3-23. Acoustic profile through Lake Proctor Core Sites P2 and P3. Core diagrams are shown at the points of closest approach on the profile. The track line of the profile is shown in Figure 3-19. Core P2 bottomed in previously dried and hardened lake sediment. The pre-impoundment surface was not reached. Core Site P2 is 37.4 ft from the profile. Core Site P3, which is 7.1 ft off the profile, bottomed in a highly compacted clay-rich soil at a shallower depth than the apparent depth to the pre-impoundment surface.

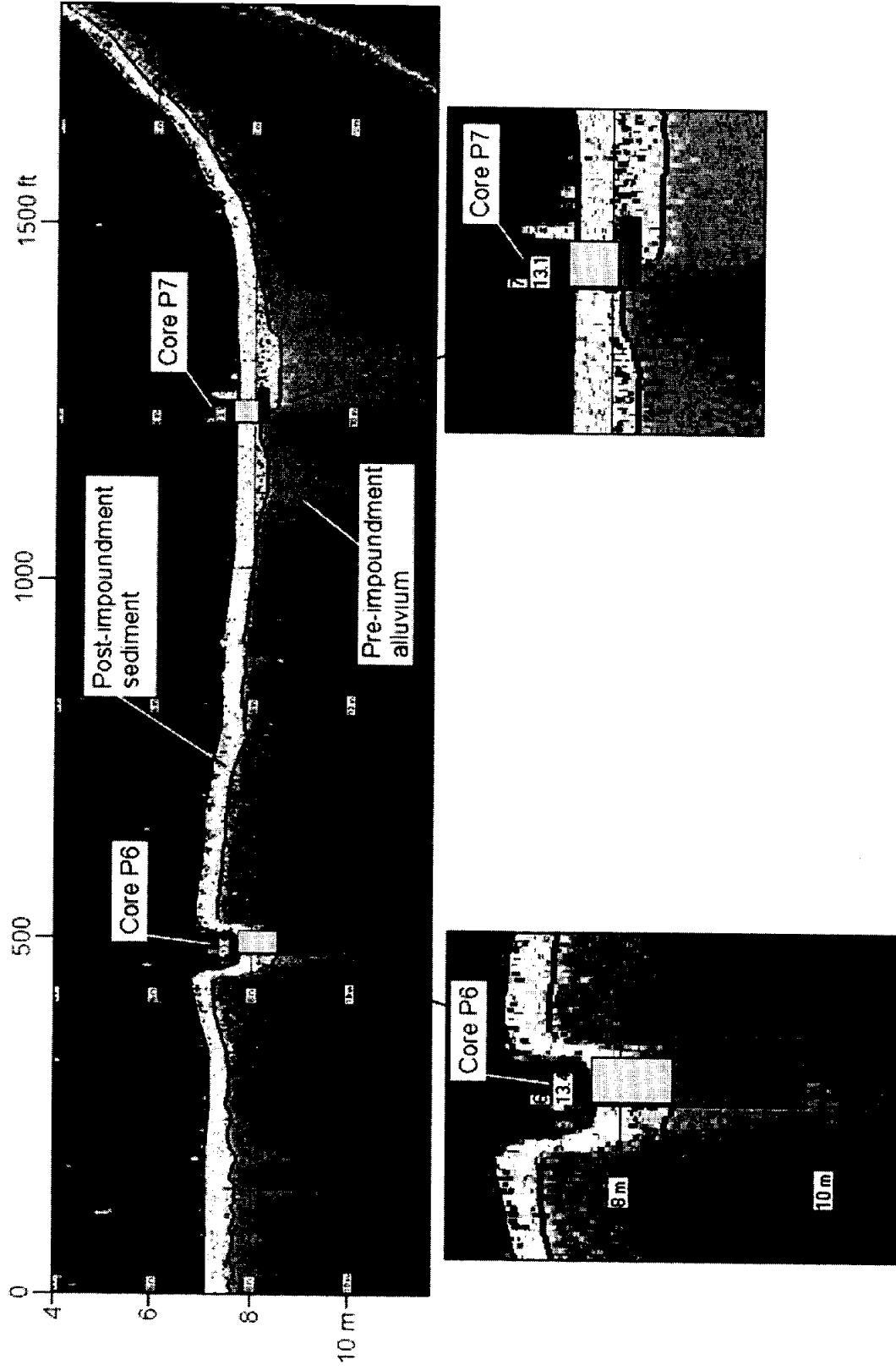


Figure 3-24. Acoustic profile through Lake Proctor Core Sites P6 and P7. Core diagrams are shown at the points of closest approach on the profile. The track line of the profile is shown in Figure 3-19. Core Site P6 is 13.4 ft from the profile. Core Site P7 is 13.1 ft from the profile. As in Aquilla Core A2c, the base of the post-impoundment sediment in Core P6 is placed at the point the water content drops below 60%. The underlying pre-impoundment at Site P6 is fluvial a deposit of similar texture.

4. Discussion

The goal of this study was to demonstrate the relationship between the thickness of post-impoundment sediments determined from coring and the acoustically determined thickness made using the SDI sub-bottom profiler in Brazos River basin Lakes Aquilla, Granger, Limestone, and Proctor. The first task was to determine the extent to which we could identify the pre-impoundment surface within the cores. We found that in the four reservoirs the pre-impoundment surface was distinct and easily identified in all the cores collected on the submerged floodplains. The pre-impoundment materials are characterized by low water content (25 to 35% water content versus 50 to 80% water content for the post-impoundment sediments), high shear strength (1 to 2 kg/cm² versus 0.05 to 0.5 kg/cm² for the post-impoundment sediment) and the common presence of tree bark, twigs and leaf litter on the pre-impoundment surface and intact plant roots within the soil immediately below the pre-impoundment surface. The distinction between pre- and post-impoundment sediment is not as great in cores collected in the submerged river channels. Generally the lake and river sediments have similar textures (percentages of sand, silt and clay) and appearance. There are contrasts in water content and shear strength, but the differences are more subtle than those found on the floodplain.

We found that the post-impoundment layer also produced a distinct acoustic response that allowed the base of lake sediments to be easily traced on acoustic profiles in all four reservoirs. The post-impoundment layer is generally 1 m or less thick and tends to thin over local bathymetric highs and thicken in local lows in all four reservoirs. In spite of the subtle differences found in the cores, the distinction between pre- and post-impoundment sediments in the river channels is clear on the acoustic records. In each case where the post-impoundment interval was present, the base of the layer is distinct on the acoustic profiles and could be traced continuously from the floodplains, across the river channels, to the opposite floodplains. In practice, the best approach may be to core the floodplain deposits to confirm the identification of the pre-impoundment surface and then trace that identified surface on the acoustic records across the river channels.

In the four reservoirs the post-impoundment sediments produce strong returns from all three acoustic frequencies generated by the SDI profiler (200, 48 and 24 kHz). This causes the post-impoundment layer to appear white to yellow, with specks of red on the three-color displays generated by the interpretation program Depthpic. In contrast, the pre-impoundment material in all four reservoirs, whether it was alluvium, colluvium, or river channel deposits, produced acoustic returns at only the lowest (24 kHz) signal frequency. Hence, pre-impoundment deposits and soils appear light to dark blue on the three-color displays. Of the three signal frequencies the distinction between pre- and post-impoundment materials was clearest on the 48 kHz data. In most cases it would be possible to map the sediment thickness based on the 48 kHz data alone, particularly in lakes Aquilla and Granger. However, in Lake Limestone near the dam and throughout Lake Proctor, the distinction between pre- and post-impoundment was clearer on the three-color displays, which combine all three signal frequencies. Hence, early in the interpretation process for a given lake it is useful to experiment with the display options in Depthpic to find the display type that shows the clearest distinction between pre- and post-impoundment materials. Although it would be possible to reliably identify and trace the base of

the post-impoundment sediments without guidance from core data, having results from coring provides a useful confirmation that the correct surface is being mapped.

Another finding of this study that applies to all four lakes is that a distinct pre-impoundment interval is clear and traceable in all four reservoirs. Like the overlying post-impoundment deposits, this pre-impoundment layer thickens in the local lows and thins over the local highs in the lake bottom bathymetry. It appears light blue on the three-color displays and black and white speckled on the 48 kHz data. The identification that the interval is pre-impoundment is based on the occurrence of tree bark and leaf litter on its upper surface and intact plant roots within it, immediately below its upper surface. We speculate that this pre-impoundment interval may correspond to what is referred to as post-settlement alluvium (Daniels and Jordan, 1966; Leece, 1997). Post-settlement alluvium is a surficial deposit on fans and floodplain surfaces that has been deposited discontinuously since cultivation of watersheds began about the 1880's. Post-settlement alluvium deposits can be in excess of 1-2 meters in thickness. They are typically deepest in close proximity to the stream channel and thin perpendicular (away from) the stream. For the purpose of estimating the loss of reservoir storage capacity due to post-impoundment sedimentation, it is critical that the distinction is correctly made between pre-impoundment deposits of this kind and the post-impoundment sediment and that the pre-impoundment interval is not included in the estimates for post-impoundment sediment volume.

Another result of the study is that the overall distribution of post-impoundment sedimentation differs from reservoir to reservoir. In both Lakes Aquilla and Limestone post-impoundment deposition is largely restricted to the submerged river channels. Only a few centimeters of sediment have accumulated in the adjacent submerged floodplains in the 20 years or more since impoundment. The thickness of the post-impoundment deposits increases in the river channel toward the middle reaches of both reservoirs, and local accumulations appear on the adjacent submerged floodplains. However, in the middle reaches the deposits on the submerged floodplains are restricted to local depressions in the old floodplain surfaces and they pick-out against local highs in the surface. Further downstream, near the dams, in both reservoirs the post-impoundment sediments are broadly deposited in a nearly uniform layer across both submerged floodplains and river channels. Lake Proctor has a different distribution of sediments. The deposition throughout Lake Proctor looks similar to that that occurs near the dams in Lakes Aquilla and Limestone. The sediments form a nearly uniform thick layer across the submerged floodplains and river channels.

One possible explanation for the difference in sediment distribution in Proctor is that the deposition pattern changes with the age of the reservoir. Lakes Aquilla and Limestone are 20 and 25 years old, respectively. Lake Proctor is 40 years old. By far, most of the sedimentation in reservoirs occurs at periods of high flow in response to storms within the supplying watershed. It is possible that when these reservoirs were first impounded that the submerged river channels acted as conduits through which sediment-laden waters from the typical storm were funneled as turbidity flows through the upstream reaches, bypassing the floodplains almost entirely. When these turbidity flows reached the dam they would spill out over the submerged floodplains and backup upstream in the channels. Hence, deposition in the young reservoir would be restricted to the river channels in the upstream reaches and broadly distributed near the dam, as observed in Lakes Aquilla and Limestone. However, with age the river channels will progressively fill with sediment to the point that the turbidity flows produced by the typical storm cannot be contained within the remaining cross-section area of the submerged river channel. When this happens the

turbidity flows will spill out onto the floodplain upstream of the dam. With time, the point at which the turbidity flows top the submerged channel in the typical storm will move up stream to the point that in a mature to old reservoir deposition occurs broadly across the submerged floodplains throughout the reservoir. The rate at which this proposed progression would occur would depend on the volume of the typical turbidity flow versus the cross-sectional area of the initial submerged river channel and its initial slope.

Although the proposed time progression could explain the different sediment distribution in Lake Proctor, a somewhat different process must be occurring in Lake Granger. In Lake Granger the deposition on the submerged floodplain follows the pattern of Lakes Aquilla and Limestone, being limited to the lows in the middle reaches and broadly distributed nearer the dam. However, the submerged channels within Lake Granger from the middle reaches to near the dam are largely devoid of post-impoundment sediment. On the profile we collected nearest the dam in Lake Granger, the post-impoundment layer forms a 75 cm high bank flanking each side of the submerged river channel (Figure 3-11). The submerged river channel contains no post-impoundment sediment. One possible explanation of the lack of deposits in the channels is that sediments deposited there during storms are later removed by dense clear-water flows down the channels. However, a study of real-time depositional processes in Lake Granger would be required to explain this phenomenon.

5. CONCLUSIONS

This study was done to determine the extent to which the base of post-impoundment sedimentation could be identified and traced on SDI profiler data and to serve as a guide for interpreting sedimentation survey data in the four reservoirs considered. The main conclusions are listed below.

1. Using the vibracore method, the pre-impoundment surface can be reached and sampled throughout the reservoirs, except in areas that have been extensively exposed and desiccated in the past. The pre-impoundment surface can be reliably identified in cores collected on the submerged floodplains from visual examination of the core, looking for plant remains on the pre-impoundment surface and intact plant roots immediately below the surface. Physical properties of the core material, particularly water content and shear strength, also aid in the identification of the pre-impoundment surface. The distinction between pre- and post-impoundment sediment in cores from the submerged river channels is subtle. Hence, the submerged floodplain in the downstream reaches of the reservoir (closest to the dam) is likely the best site to sample post-impoundment sediment and to confirm the identification of the pre-impoundment surface on the acoustic data. Spud bars can be used for general sediment thickness estimates, but in silty sediments they can significantly underestimate the post-impoundment sediment thickness.
2. The post-impoundment layer is distinct and traceable on all acoustic profiles collected with the SDI multi-frequency profiling system in all four reservoirs. On the three-color displays produced by the interpretation program Depthpic, the post-impoundment layer appears white to yellow with specks of red. The underlying pre-impoundment materials appear light to dark blue. In most places on the 48 kHz data, the post-impoundment layer appears light gray, almost transparent, and the underlying pre-impoundment materials appear black and

white speckled. Using these criteria, the pre-impoundment surface is distinct and traceable across all profiles. In the direct comparisons between short acoustic records and core results, the acoustic data correlated best with the core data using a sediment velocity of 1440 m/s (4,723 ft/s). This velocity is consistent with velocities of near-bottom silty-clay sediments and similar to the velocity of sediment determined in Lake Waco (Dunbar et al., 1999).

3. Given the consistency of results from the four reservoirs considered, plus the range of sediment textures, geology of the supplying watersheds, and reservoir age, it would be possible to identify and map the post-impoundment layer based on the acoustic data alone in future sediment surveys of similar reservoirs in the Brazos River basin. A more conservative and reliable approach would be to augment future sediment surveys with a limited coring program (1 to 3 cores), targeting the downstream floodplains, to verify the identification of the pre-impoundment surface. Once confirmed and correlated with acoustic data as shown in this study, the pre-impoundment surface could be traced throughout the reservoir based on the acoustic data alone.

6. REFERENCES

Bennett, S. J. and J. A. Dunbar, 2003. Physical and stratigraphic characteristics of sediments impounded within a flood control reservoir in Oklahoma, Transactions of the American Society of Agricultural Engineers, v 46, p. 269-277.

Bennett, S. J., and F. E. Rhoton, 2003. Physical and chemical characteristics of sediment impounded within Grenada Lake, MS. USDA-ARS National Sedimentation Laboratory Research Report No. 36, 161pp.

Binford, M.W., and M. Brenner, 1986. Dilution of ^{210}Pb by organic sedimentation in lakes of different trophic states, and application to studies of sediment-water interactions. Limnology and Oceanography, 31, 584-595.

Daniels, R. and Jordan, R.H., 1966. Physiographic history and the soils enterenched stream systems, and gullies, Harrison County, Iowa. U.S.D.A. Technical Bulletin 1348. 116p.

Dunbar, J. A., P. M Allen, and S. J. Bennett, Acoustic Imaging of Sediment Impounded by a USDA-NRCS Flood Control Dam, Oklahoma, USDA Research Report No. 22, National Sedimentation Laboratory Channel and Watershed Processes Research Unit, Oxford, Mississippi 38655, 54 p., September, 2001.

Dunbar, J.A., P.M. Allen, and P.D. Higley, 1999. Multifrequency acoustic profiling for water reservoir sedimentation studies. Journal of Sedimentary Research, 69, 521-527.

Dunbar, J. A., S. J. Bennett, P. D. Higley, and F. E. Rhoton. 2003, Sedimentation patterns within a flood control reservoir: Grenada Lake, MS, USDA-ARS, Research Report No. 38, USDA National Sedimentation Laboratory, Oxford Mississippi.

Johnson, W.C., Cantwell, H.D., Dean, T., 1980. The impact of agricultural settlement on Canadian Sandy Creek, Oklahoma. *Proc. Oklahoma Academy of Science*, 60:82-88.

Lanesky, D.E., B.W. Logan, R.G. Brown, and A.C. Hine, 1979. A new approach to portable vibracoring underwater and on land. *Journal of Sedimentary Petrology*, 49, 654-657.

Leece, S.A. 1997. Spatial patterns of historical overbank sedimentation and floodplain evolution, Blue River, Wisconsin. *Geomorphology* 18:265-277.

Ritchie, J.C., and J.R. McHenry, 1990. Application of radioactive fallout Cesium-137 for measuring soil erosion and sediment accumulation rates and patterns: A review. *Journal of Environmental Quality*, 19, 215-233.

Smith, D.G., 1984. Vibracoring fluvial and deltaic sediments: Tips on improving penetration and recovery. *Journal of Sedimentary Petrology*, 54, 660-663.

Appendix A: Physical Analysis of Cores

Aquilla	Core 1		Spud 0.6 ft					
Sample	Top (cm)	Bot (cm)	Cont. wt (gr)	Wet wt. (gr)	Dry wt. (gr)	Wat Cont. (%)	Shear	Comment 1
1	0	5	8.25	277.02	114.28	60.5	0	
2	5	10	8.34	285.93	197.74	31.8	1.8	Pre-impoundment
3	10	15	7.89	317.15	228.84	28.6	3.4	

Aquilla	Core 2C							
Sample	Top (cm)	Bot (cm)	Con. Wt (gr)	Wet wt. (gr)	Dry wt. (gr)	Wat Cont. (%)	Shear (kg)	Comment 1
1	0	5	8.65	208.27	57.07	75.7	0	
2	5	10	8.08	150.76	48.81	71.5	0	
3	10	15	8.4	228.03	78.38	68.1	0	
4	15	20	8.56	295.94	106.12	66.1	0	
5	20	25	8.05	213.49	79.89	65.0	0	
6	25	30	8.3	255.33	96.09	64.5	0	
7	30	35	8.42	235.91	92.35	63.1	0	
8	35	40	8.31	242.9	96.27	62.5	0.1	
9	40	45	7.95	280.15	112.29	61.7	0.05	
10	45	50	8.31	250.19	108.44	58.6	0.2	
11	50	55	8.3	290.81	117.24	61.4	0.15	
12	55	60	8.45	190.37	77.85	61.9	0.15	
13	60	65	8.29	247.8	104.68	59.8	0.15	
14	65	70	8.19	272.65	118.12	58.4	0.3	
15	70	75	8	250.79	99.28	62.4	0.4	
16	75	80	8.18	233.88	94.11	61.9	0.4	
17	80	85	8.25	247.95	102.44	60.7	0.6	
18	85	90	8.09	259.17	102.74	62.3	0.4	
19	90	95	7.93	275.93	109.6	62.1	0.4	
20	95	100	8.54	251.34	98.24	63.1	0.35	
21	100	105	8.67	208.51	86.18	61.2	0.4	
22	105	110	8.44	272.12	114.34	59.8	0.6	
23	110	115	8.52	270.22	111.01	60.8	0.6	
24	115	120	8.37	203.03	84.86	60.7	0.6	
25	120	125	8.54	265.7	107.88	61.4	0.6	
26	125	130	8.41	264.46	110.53	60.1	0.7	
27	130	135	8.32	274.81	112.56	60.9	0.6	
28	135	140	8.31	295.42	121.94	60.4	0.6	
29	140	145	8.28	254.95	104.51	61.0	0.6	
30	145	150	8.28	247.57	103.94	60.0	0.6	
31	150	155	8.42	261.8	109.18	60.2	0.7	
32	155	160	8.35	262.34	162	39.5	0.7	
33	160	165	8.09	279.13	176.89	37.7	0.7	
34	165	170	8.02	275.81	169.75	39.6	0.8	
35	170	175	8.02	248.51	120.19	53.4	0.8	
36	175	180	8.32	277.36	130.07	54.7	0.9	
37	180	185	7.88	262.3	192.35	27.5	0.8	
38	185	190	7.84	253.75	186.11	27.5	0.8	

39	190	195	7.83	260.68	142.17	46.9	1
40	195	200	7.93	306.23	144.32	54.3	1.1
41	200	205	8.02	249.64	115.36	55.6	1.1
42	205	210	8.03	294.24	139.89	53.9	1.1
43	210	215	8.07	293.16	139.51	53.9	1.2
44	215	220	8.33	292.5	131.55	56.6	1.3
45	220	225	8.44	269.38	144.01	48.0	1.2
46	225	230	8.43	267.95	141.71	48.6	1.5
47	230	235	8.3	268.74	123.39	55.8	1.4
48	235	240	8.45	284.02	133.53	54.6	1.2
49	240	245	8.65	319.28	149.63	54.6	1.4
50	245	250	8.17	272.15	122.02	56.9	1.4
51	250	255	8.35	236.46	152.63	36.7	1.2 dark organic
52	255	260	8.46	273.64	159.96	42.9	1 end of organic
53	260	265	7.91	326.72	175.43	47.5	1.5
54	265	270	8.14	248.81	131.24	48.9	1.1
55	270	275	8.05	283.88	157.84	45.7	1.3
56	275	280	8.05	265	148.46	45.4	1.5 Granular
57	280	285	8.01	298	173.63	42.9	1.8 Granular
58	285	290	8.34	249.32	145.11	43.2	1.8 Fill floor?
59	290	295	8.32	296.35	171.14	43.5	1.8
60	295	300	8.38	248.35	181.43	27.9	3.5
61	300	305	7.82	299.17	235.38	21.9	11 Rock frags & Pebble

Aquilla	Core 3a		Spud 2.3 ft					
Sample	Top (cm)	Bot (cm)	Cont. wt (gr)	Wet wt. (gr)	Dry wt. (gr)	Wat Cont. (%)	Shear (kg)	Comment 1
1	0	5	8.15	230.38	50.93	80.7	0	
2	5	10	8.25	283.17	74.55	75.9	0	
3	10	15	8.25	242.87	72.91	72.4	0	
4	15	20	8.18	238.02	76.3	70.4	0.25	
5	20	25	8.17	289.27	102.94	66.3	0.25	
6	25	30	8.17	271.38	94.35	67.3	0.3	
7	30	35	7.89	267.58	94.69	66.6	0.25	
8	35	40	8.24	245.24	92.66	64.4	0.4	
9	40	45	8.32	291.33	113.16	63.0	0.35	
10	45	50	8.18	260.91	107.82	60.6	0.45	
11	50	55	8.33	274.17	139.76	50.6	0.4	54 cm to pre-imp.
12	55	60	8.18	372.05	261.05	30.5	6.4	
13	60	65	7.94	343.44	248.23	28.4	7.8	
14	65	70	7.8	176	129.45	27.7	7.2	

Aquilla	Core 4		Spud 0.6 ft					
Sample	Top (cm)	Bot (cm)	Cont. wt (gr)	Wet wt. (gr)	Dry wt. (gr)	Wat Cont. (%)	shear (kg)	Comment 1
1	0	5	7.95	275.4	115.06	60.0	0	
2	5	10	8.17	286	166.22	43.1	0.05	1 cm of Pre-imp.
3	10	15	8.1	361.19	263.95	27.5	4.1	Pre-impoundment
4	15	19	7.91	314.81	234.51	26.2	4.35	

Aquilla	Core 5		Spud 1.1 ft						
Sample	Top (cm)	Bot (cm)	Cont. wt (gr)	Wet wt. (gr)	Dry wt. (gr)	Wat Cont. (%)	Shear (kg)	Comment 1	
1	0	5	8.31	226.28	73.9	69.9	0		
2	5	10	7.87	245.69	86.7	66.9	0.4		
3	10	15	8.28	227.47	88.46	63.4	0.1		
4	15	20	7.86	278.02	112.82	61.1	0.25		
5	20	25	8.28	298.41	121.2	61.1	0.25		
6	25	30	7.9	270.75	115.16	59.2	0.2		
7	30	35	7.92	311.27	144.36	55.0	0.2		
8	35	40	7.81	308.46	157.79	50.1	0.3		
9	40	45	8.29	258.72	132.35	50.5	0.3		
10	45	50	7.88	278.75	158.05	44.6	0.45		
11	50	55	7.86	411.8	286.88	30.9		3	Pre-impoundment
12	55	60	7.83	361.39	257.46	29.4	2.4		
13	60	65	8.27	336.08	245.88	27.5	1.8	roots	
14	65	70	7.9	311.6	229.57	27.0	2.4		
15	70	75	7.89	401	303.52	24.8	4.2		

Aquilla	Core 6		Spud 1.2 ft		Len 67 cm				
Sample	Top (cm)	Bot (cm)	Cont. wt (gr)	Wet wt. (gr)	Dry wt. (gr)	Wat Cont. (%)	Shear (kg)	Comment 1	
1	0	5	8.39	289.98	67.44	79.0	0		
2	5	10	8.35	256.37	68.66	75.7	0		
3	10	15	8.18	216.21	61.22	74.5	0		
4	15	20	8.4	281.26	82.76	72.7	0		
5	20	25	8.47	296.86	88.52	72.2	0		
6	25	30	8.2	237.3	71.44	72.4	0.05		
7	30	35	8.23	241.08	74.79	71.4	0		
8	35	40	8.19	212.38	64.49	72.4	0		
9	40	45	8.54	291.91	96.87	68.8	0		
10	45	50	8.55	269.49	105.13	63.0	0.1		
11	50	55	8.34	332.78	153.3	55.3	0.1		
12	55	57	8.15	155.02	97.03	39.5	0.6	roots/black soil	

Granger	Core 1a								
Sample	Top (cm)	Bot (cm)	Cont. wt (gr)	Wet wt. (gr)	Dry wt. (gr)	Wat Cont. (%)	Shear (kg)	Comment 1	
1	0	5	8.25	213.18	76.03	66.9	0		
2	5	10	8.13	301.35	120.21	61.8		0	dark gray, clay
3	10	15	8.35	307.09	136.84	57.0	0.1		
4	15	20	8.07	239.53	111.61	55.3		0.2	above 29 cm is
5	20	25	7.86	341.56	168.68	51.8		0.1	dark gray, clay
6	25	30	8.3	267.41	167.05	38.7		0.4	At 29 cm hit top
7	30	35	8.3	259.45	211.48	19.1		5.4	of light gray to tan
									layer - silty
									with no roots

Granger	Core 2a		Spud 7 ft				
Sample	Top (cm)	Bot (cm)	Cont. wt (gr)	Wet wt. (gr)	Dry wt. (gr)	Wat Cont. (%)	Shear (kg)
1	0	5	8.3	304.3	98.97	69.4	0
2	5	10	8.24	328.72	110.02	68.2	0
3	10	15	8.2	219.61	77.17	67.4	0
4	15	20	7.92	275.81	100.53	65.4	0
5	20	25	8.16	249.54	89.98	66.1	0
6	25	30	8.26	287.68	104.43	65.6	0.1
7	30	35	8.19	248.68	93.4	64.6	0.1
8	35	40	8.27	325.08	121.93	64.1	0.2
9	40	45	8.37	216.67	82.68	64.3	0.15
10	45	50	8.29	282.93	105.74	64.5	0.25
11	50	55	8.25	302.13	116.83	63.1	0.35
12	55	60	8.19	296.98	124.27	59.8	0.4
13	60	65	8.29	278.24	119.68	58.7	0.4
14	65	70	8.07	245.13	105.41	58.9	0.6
15	70	75	8.33	298.5	138.32	55.2	0.55
16	75	80	8.17	201.07	98.79	53.0	0.6
17	80	85	8.02	360.69	206.28	43.8	5.1
18	85	90	8.16	255.58	170.07	34.6	5.5
19	90	95	8.26	342.72	236.4	31.8	4.6

Granger	Core 3						
Sample	Top (cm)	Bot (cm)	Cont. Weight	Wet wt. (gr)	Dry wt. (gr)	Wat Cont %	Shear (kg)
1	0	5	8.29	304.52	76.16	77.1	0
2	5	10	8.29	208.08	71.47	68.4	0
3	10	15	8.41	211.49	94.79	57.5	0
4	15	20	8.25	214.13	78.85	65.7	0
5	20	25	8.23	235.4	86.22	65.7	0
6	25	30	8.42	210.58	80.08	64.6	0.05
7	30	35	8.37	161.07	63.31	64.0	0.1
8	35	40	8.34	243.43	92.52	64.2	0.15
9	40	45	8.4	250.08	96.3	63.6	0.1
10	45	50	8.32	216.87	86.86	62.3	0.2
11	50	55	8.17	234.11	93.56	62.2	0.2
12	55	60	8.38	236.49	91.75	63.5	0.15
13	60	65	8.14	213.22	84.84	62.6	0.2
14	65	70	8.18	246.52	96.87	62.8	0.2
15	70	75	8.19	261.23	104.89	61.8	0.4
16	75	80	8.32	235.84	93.71	62.5	0.4
17	80	85	8.41	282.31	114.4	61.3	0.6
18	85	90	8.42	190.34	83.17	58.9	0.9
19	90	95	8.4	260.71	111.31	59.2	0.9
20	95	100	8.92	216.79	91.32	60.4	0.9
21	100	105	8.43	270.48	113.05	60.1	0.65
22	105	110	8.32	324.24	135.3	59.8	0.65
23	110	115	8.06	257.5	105.67	60.9	0.7
24	115	120	8.13	260.79	101.31	63.1	0.7

25	120	125	8.39	269.9	108	61.9	0.6
26	125	130	8.14	241.82	97.75	61.7	0.6
27	130	135	8.51	294.77	120.45	60.9	0.6
28	135	140	8.83	279.14	122.16	58.1	0.6
29	140	145	8.29	261.31	111.47	59.2	0.7
30	145	150	8.34	286.04	116.56	61.0	0.7
31	150	155	8.29	195.39	80.77	61.3	0.75
32	155	160	8.57	318.52	131.32	60.4	0.7
33	160	165	8.4	244.02	103.22	59.8	0.8
34	165	170	8.33	253.75	111.18	58.1	0.85
35	170	175	8.24	249.27	110.93	57.4	0.9
36	175	180	8.4	229.99	101.57	58.0	1
37	180	185	7.98	269.02	116.55	58.4	0.9
38	185	190	8.61	227.83	102.51	57.2	0.8
39	190	195	8.23	284.34	129.42	56.1	1.1
40	195	200	8.41	211.87	96.38	56.8	0.9
41	200	205	8.29	209.46	93.2	57.8	0.5

Granger	Core 4							
Sample	Top (cm)	Bot (cm)	Cont. Weight	Wet wt. (gr)	Dry wt. (gr)	Wat Cont %	Shear (kg)	Comment
1	0	5	8.35	276.6	117.87	59.2	0.05	
2	5	10	8.28	345.1	167.61	52.7	0.1	
3	10	15	8.36	309.65	174.94	44.7	0.5	
4	15	20	7.99	266.8	174.12	35.8	0.9	
5	20	25	7.99	393.03	273.82	31.0	2	Dark Gray
								Tree bark
								Roots

Granger	Core 5							
Sample	Top (cm)	Bot (cm)	Cont. Weight	Wet wt. (gr)	Dry wt. (gr)	Wat Cont %	Shear (kg)	Comment
1	0	5	7.94	301.45	104.87	67.0	0	
2	5	10	8.19	268.97	103.34	63.5	0	
3	10	15	8.4	276.17	111.92	61.3	0.1	
4	15	20	8.26	287.87	121.25	59.6	0.1	
5	20	25	8.22	281.56	121.31	58.6	0.2	
6	25	30	8.31	288.93	127.05	57.7	0.2	
7	30	35	8.39	299.5	136.75	55.9	0.35	
8	35	40	8.32	281.74	153.84	46.8	0.8	1 cm of fill
9	40	45	8.41	314.84	218.47	31.4	3.5	Twigs, roots

Granger	Core 3							
Sample	Top (cm)	Bot (cm)	Cont. Weight	Wet wt. (gr)	Dry wt. (gr)	Wat Cont %	Shear (kg)	
1	0	5	8.26	197.17	60.69	72.2	0	
2	5	10	7.94	266.84	89.56	68.5	0	
3	10	15	8.28	171.59	99.9	43.9	0	
4	15	20	8.14	241	87.08	66.1	0	
5	20	25	8.2	239.56	87.82	65.6	0	
6	25	30	8.34	286.21	102.79	66.0	0.05	
7	30	35	8.4	215.24	79.46	65.6	0.05	
8	35	40	8.28	244.31	87.32	66.5	0	
9	40	45	8.13	261.66	99.42	64.0	0.1	
10	45	50	8.4	232.29	90.31	63.4	0.1	
11	50	55	8.21	237.95	92.03	63.5	0.1	
12	55	60	8.4	222.16	88.25	62.6	0.1	
13	60	65	8.32	299.75	120.99	61.3	0.3	
14	65	70	8.28	231.65	93.26	62.0	0.3	
15	70	75	8.32	263.22	107.98	60.9	0.3	
16	75	80	8.3	276.63	116.3	59.8	0.45	
17	80	85	8.26	273.31	112.8	60.6	0.5	
18	85	90	8.24	255.56	108.13	59.6	0.45	
19	90	95	8.3	250.51	105.73	59.8	0.45	
20	95	100	8.5	246.7	100.59	61.3	0.45	
21	100	105	8.17	287.85	116.34	61.3	0.45	
22	105	110	8.22	239.4	102.6	59.2	0.65	
23	110	115	7.93	301.45	121.42	61.3	0.6	
24	115	120	8.16	265.69	109.5	60.6	0.5	
25	120	125	8.19	265.57	109.2	60.8	0.65	
26	125	130	8.17	254.06	106.73	59.9	0.6	
27	130	135	8.42	261.21	110.68	59.5	0.7	
28	135	140	8.13	279.98	115.59	60.5	0.7	
29	140	145	8.42	276.77	117	59.5	0.7	
30	145	150	8.18	273.81	119.62	58.0	0.65	
31	150	155	8.29	296.49	128.64	58.2	0.8	
32	155	160	8.3	266.47	115.66	58.4	0.8	
33	160	165	8.21	221.2	97.82	57.9	0.8	
34	165	170	8.19	267.67	115.99	58.5	0.95	
35	170	175	7.91	292.5	123.69	59.3	0.85	
36	175	180	8.25	264.43	116.65	57.7	0.95	
37	180	185	8.18	268.24	111.55	60.3	0.9	
38	185	190	8.28	255.67	106.62	60.2	0.9	
39	190	195	8.26	286.6	124.22	58.3	0.9	
40	195	200	8.26	300.82	128.73	58.8	0.8	
41	200	205	8.18	278.98	120.04	58.7	0.95	
42	205	210	8.27	245.82	106.3	58.7	0.95	
43	210	215	8.04	269.55	122.47	56.2	0.95	
44	215	220	8.33	275.68	124.73	56.5	0.85	
45	220	225	8.17	259.85	122.1	54.7	1	

Limestone	Core 1b							
Sample	Top (cm)	Bot (cm)	Cont. Weight	Wet wt. (gr)	Dry wt. (gr)	Wat Cont %	Shear (kg)	Comment
1	0	5	8.14	220.96	43.28	83.5	0	
2	5	10	7.94	151.8	34.58	81.5	0	
3	10	15	8.17	233.58	54.79	79.3	0	
4	15	20	8.07	231.88	61.27	76.2	0	
5	20	25	8.29	248.41	72.82	73.1	0	
6	25	30	7.98	257.38	77.04	72.3	0.1	
7	30	35	8.22	243.58	76.1	71.2	0.15	
8	35	40	8.29	219.25	69.02	71.2	0.2	
9	40	45	8.3	295.98	94.81	69.9	0.2	
10	45	50	8	257.14	80.7	70.8	0.1	
11	50	55	8.06	261.47	78.6	72.2	0.15	
12	55	60	8.3	217.63	68.49	71.2	0.1	
13	60	65	7.83	255.57	81.56	70.2	0.15	
14	65	70	8.16	246.57	81.48	69.2	0.15	
15	70	75	8.43	252.05	87.02	67.7	0.2	
16	75	80	8.34	282.27	107.08	64.0	0.4	
17	80	85	8.21	256.28	109.98	59.0	0.3	
18	85	90	8.26	262.97	130.71	51.9	0.45	
19	90	95	8.17	343.94	226.46	35.0	0.9	Tree bark,
20	95	100	8.53	369.3	242.81	35.1	2.7	roots, silt

Limestone	Core 2a		spud 0.6 ft					
Sample	Top (cm)	Bot (cm)	Cont. Weight	Wet wt. (gr)	Dry wt. (gr)	Wat Cont %	Shear (kg)	Comment
1	0	5	8.18	265.43	80.75	71.8	0	
2	5	10	8.15	282.42	151.93	47.6	0.9	9 cm of post-imp.
3	10	15	8.15	274.91	186.96	33.0	6.8	
4	15	17	8.26	173.03	117.08	34.0	7.5	Small roots

Limestone	Core 3a						
Sample	Top (cm)	Bot (cm)	Cont. wt (gr)	Wet wt. (gr)	Dry wt. (gr)	Wat Cont. (%)	Shear (kg)
1	0	5	8.17	171.09	33.13	84.7	0
2	5	10	8.29	223.68	49.19	81.0	0
3	10	15	8.24	224.67	53.71	79.0	0
4	15	20	7.95	253.62	65.63	76.5	0
5	20	25	7.87	242.38	66.25	75.1	0
6	25	30	8.34	250	72.23	73.6	0
7	30	35	8.09	246.93	73.02	72.8	0.15
8	35	40	8.32	236.89	70.45	72.8	0.25
9	40	45	8.25	258.57	81.01	70.9	0.25
10	45	50	8.22	253.86	80.97	70.4	0.3
11	50	55	8.16	261.67	83.61	70.2	0.35
12	55	60	8.28	237.14	77.97	69.5	0.35

13	60	65	8.26	268.19	88.08	69.3	0.4
14	65	70	8.22	279.23	96.67	67.4	0.5
15	70	75	8.3	247.79	85.16	67.9	0.5
16	75	80	8.19	264.94	87.93	68.9	0.5
17	80	85	8.3	261.94	84.88	69.8	0.5
18	85	90	8.1	265.16	89.18	68.5	0.55
19	90	95	8.18	246.29	91.36	65.1	0.5
20	95	100	8.18	250.84	88.32	67.0	0.7
21	100	105	8.29	256.88	90.66	66.9	0.5
22	105	110	8.26	285.8	101.06	66.6	0.6
23	110	115	8.28	247.89	90.87	65.5	0.7
24	115	120	8.05	253.42	94.32	64.8	0.65
25	120	125	8.05	265.01	103.69	62.8	0.7
26	125	130	7.84	298.42	106.12	66.2	0.75
27	130	135	8.25	259.67	101.47	62.9	0.8
28	135	140	8.38	282.41	108.22	63.6	0.8
29	140	145	7.94	252.57	102.01	61.5	0.7
30	145	150	8.15	325.71	134.74	60.1	0.65
31	150	155	8	238.81	97.44	61.2	0.65
32	155	160	8.01	277.01	120.53	58.2	0.9
33	160	165	8.23	282.38	135.62	53.5	0.9
34	165	170	8.55	366.28	182.98	51.2	0.9

Limestone	Core 4							
Sample	Top (cm)	Bot (cm)	Cont. Weight	Wet wt. (gr)	Dry wt. (gr)	Wat Cont %	Shear (kg)	Comment
1	0	5.5	8.37	372.97	257.06	31.8	5.2	gras blades twigs, leaves roots

Limestone	Core 5a							
Sample	Top (cm)	Bot (cm)	Cont. Weight	Wet wt. (gr)	Dry wt. (gr)	Wat Cont %	Shear (kg)	Comment 1
1	0	5	8.26	212.08	42.63	83.1	0	
2	5	10	8.14	239.61	52.76	80.7	0	
3	10	15	8.15	256.52	61.21	78.6	0	
4	15	20	8.31	238.42	61.77	76.8	0	
5	20	25	8.29	256.13	69.73	75.2	0.1	
6	25	30	8.21	233.09	65.37	74.6	0.15	
7	30	35	8.23	264.33	76.8	73.2	0.1	
8	35	40	8.25	271.92	76.83	74.0	0.2	
9	40	45	8.34	214.21	62.35	73.8	0.15	
10	45	50	8.35	283.26	86.21	71.7	0.2	
11	50	55	8.28	210.43	68.82	70.1	0.3	
12	55	60	8.33	246.7	80.81	69.6	0.4	59 cm post-imp
13	60	65	8.28	222.14	76.81	68.0	0.4	Roots, Pine bark
14	65	70	7.98	269.02	94.63	66.8	0.45	
15	70	75	8.26	261.2	97.86	64.6	0.5	
16	75	80	7.86	298.5	124.12	60.0	0.5	
17	80	85	8.02	302.79	177.58	42.5	3.4	

18	85	90	8.24	377.99	280.5	26.4	8.4
19	90	95	8.15	403.9	318.22	21.7	5.9
20	95	100	7.99	361.9	258.8	29.1	3.4
21	100	105	8.22	326.35	218.57	33.9	6.6
22	105	109	8.31	297.41	229.92	23.3	7

Proctor	Core 1a		Spud 1.1 ft					
Sample	Top (cm)	Bot (cm)	Cont. wt (gr)	Wet wt. (gr)	Dry wt. (gr)	Wat Cont. (%)	Pen. At Top (kg/25)	Comment 1
1	0	5	8.16	253.85	131.2	49.9		0.4 cm soft clay
2	5	10	8.17	358.87	225.74	38.0		6.2 clay-silt
3	10	15	8.2	322.51	198.55	39.4		7.9 cracks in black
4	15	20	8.17	342.4	199.76	42.7		5.5 matrix filled with
5	20	25	7.94	301.36	176.95	42.4		2.7 tan material
6	25	30	7.99	371.46	219.16	41.9		1.8
7	30	35	8.1	330.9	220.06	34.3		6.3 Roots
8	35	40	8.12	329.63	240.63	27.7		11.3 soil
9	40	45	8.14	369.37	265.15	28.9		10.4

Proctor	Core 2		Spud 0.5 ft		Len 13 cm			
Top (cm)	Bot (cm)	Cont. wt (gr)	Wet wt. (gr)	Dry wt. (gr)	Wat Cont. (%)	Shear (kg)	Comment 1	
0	5	8.29	349.03	218.55	38.3	0.2	No clear Pre-imp.	
5	10	8.31	338.43	235.65	31.1	8.15		
10	13	8.29	210.17	143.92	32.8	9.1		

Proctor	Core 3		Spud 1.2 ft		Len 67 cm			
Sample	Top (cm)	Bot (cm)	Cont. wt (gr)	Wet wt. (gr)	Dry wt. (gr)	Wat Cont. (%)	Shear (kg)	Comment
1	0	5	8.15	230.38	50.93	80.7	0	
2	5	10	8.25	283.17	74.55	75.9	0	organic rich
3	10	15	8.25	242.87	72.91	72.4	0	
4	15	20	8.18	238.02	76.3	70.4	0.25	
5	20	25	8.17	289.27	102.94	66.3	0.25	
6	25	30	8.17	271.38	94.35	67.3	0.3	
7	30	35	7.89	267.58	94.69	66.6	0.25	
8	35	40	8.24	245.24	92.66	64.4	0.4	
9	40	45	8.32	291.33	113.16	63.0	0.35	
10	45	50	8.18	260.91	107.82	60.6	0.45	
11	50	55	8.33	274.17	139.76	50.6	0.4	top 4 cm is fill, .
12	55	60	8.18	372.05	261.05	30.5	6.4	54 cm to pre-imp
13	60	65	7.94	343.44	248.23	28.4	7.8	
14	65	67	7.8	176	129.45	27.7	7.2	

Proctor	Core 5							
Sample	Top (cm)	Bot (cm)	Cont. wt (gr)	Wet wt. (gr)	Dry wt. (gr)	Wat Cont. (%)	Shear (kg)	Comment
1	0	5	8.02	321.43	249.87	22.8	1.24	cm fill
2	5	10	8.19	300.9	240.59	20.6	3	twigs
3	10	15	8.37	303.99	243.84	20.3	2.5	tan to black
4	15	20	8.44	317.08	258.13	19.1	7.4	twigs

Proctor	Core 6							
Sample	Top (cm)	Bot (cm)		Wet (gr)	Dry wt. (gr)	Wat Cont. (%)	Shear (kg)	
1	0	5	8.36	224.8	65.02	73.8	0	
2	5	10	8.37	267.11	90.14	68.4	0	
3	10	15	8.34	248.13	82.79	69.0	0	
4	15	20	8.25	281.39	92.13	69.3	0	
5	20	25	8.39	234.08	76.52	69.8	0.1	
6	25	30	8.28	170.16	60.72	67.6	0.1	
7	30	35	8.48	272.62	97.79	66.2	0.1	
8	35	40	8.34	164.5	62.01	65.6	0.1	
9	40	45	8.32	273.27	101.31	64.9	0.15	
10	45	50	8.27	229.57	85.4	65.1	0.15	
11	50	55	8.41	216.1	85.75	62.8	0.15	
12	55	60	8.35	237.21	96.98	61.3	0.2	
13	60	65	8.4	255.43	99.98	62.9	0.25	
14	65	70	8.37	200.74	99.4	52.7	0.3	
15	70	75	8.38	231.41	95.96	60.7	0.4	
16	75	80	8.61	318.92	128.84	61.3	0.4	
17	80	85	8.33	267.6	114.19	59.2	0.5	
18	85	90	8.41	235.22	112.97	53.9	0.6	
19	90	95	8.35	283.69	139.5	52.4	0.6	
20	95	100	8.27	313.56	183.3	42.7	0.9	
21	100	105	8.5	288.52	171.15	41.9	0.85	
22	105	110	8.15	330.8	200.54	40.4	0.9	
23	110	115	8.48	271.15	160.64	42.1	1	
24	115	120	8.23	353.71	221.25	38.3	1	
25	120	125	8.45	339.86	215.46	37.5	1	
26	125	130	8.96	341.91	215.16	38.1	1.15	
27	130	135	8.44	320.91	199.14	39.0	1.2	
28	135	140	8.41	383.95	252.89	34.9	1.1	
29	140	145	8.33	324.82	210.47	36.1	1.3	
30	145	150	8.66	364.76	264.35	28.2	1.25	
31	150	155	8.61	379.02	264.76	30.8	1.15	
32	155	160	8.39	312.22	217.48	31.2	1.15	
33	160	165	8.4	340.79	243.66	29.2	1.1	
34	165	170	8.42	327.32	240.68	27.2	1.85	
35	170	175	8.41	247.62	177.43	29.3	1.7	
36	175	180	8.03	293.15	206.33	30.5	1.8	
37	180	185	8.32	283.14	207.66	27.5	1.5	

38	185	190	8.13	316.8	242.74	24.0	1.9
39	190	195	8.13	357.35	258.31	28.4	1.8
40	195	200	8.29	322.27	230.97	29.1	2
41	200	205	8.55	356.67	243.6	32.5	1.7
42	205	210	7.96	349.28	230.94	34.7	1.7
43	210	215	8.2	357.21	233.31	35.5	1.8
44	215	220	8.24	309.63	195.7	37.8	1.8
45	220	225	8.33	369.82	248.31	33.6	1.6
46	225	230	8.38	323.43	197.03	40.1	1.5
47	230	235	8.44	318.9	168.01	48.6	1.1
48	235	240	8.31	276.04	153.7	45.7	1.5
49	240	245	8.42	285.34	148.69	49.3	1.45
50	245	250	8.25	235.37	142.67	40.8	1.6
51	250	255	8.41	349.14	201.78	43.2	1.5
52	255	260	8.44	259.54	159.48	39.8	1.6
53	260	265	8.32	337.71	226.47	33.8	1.4

Proctor	Core 7							
Sample	Top (cm)	Bot (cm)	Con.(gr)	Wet (gr)	Dry wt. (gr)	Wat Cont. (%)	Shear (kg)	Comment
1	0	5	8.28	252.35	68.98	75.1	0	
2	5	10	8.19	310.69	91.51	72.5	0	
3	10	15	8.13	253.76	79.28	71.0	0	
4	15	20	8.37	265.07	89.59	68.4	0.1	
5	20	25	8.25	294.14	104.33	66.4	0.2	
6	25	30	8.36	295.76	112.32	63.8	0.15	
7	30	35	8.43	264.35	111.98	59.5	0.2	
8	35	40	8.29	275.34	128.34	55.0	0.4	
9	40	45	8.34	355.96	208.39	42.5	0.5	
10	45	50	8.11	397.43	268.29	33.2	1.7	Twigs,silt
11	50	55	8.4	298.9	222.76	26.2	2.5	twigs,roots
12	55	60	8.22	294.93	219.91	26.2	2.5	roots,silt